

1965

# Fatigue tests of welded plate girders in bending

Joseph A. Corrado  
*Lehigh University*

Follow this and additional works at: <https://preserve.lehigh.edu/etd>



Part of the [Civil Engineering Commons](#)

---

## Recommended Citation

Corrado, Joseph A., "Fatigue tests of welded plate girders in bending" (1965). *Theses and Dissertations*. 3294.  
<https://preserve.lehigh.edu/etd/3294>

This Thesis is brought to you for free and open access by Lehigh Preserve. It has been accepted for inclusion in Theses and Dissertations by an authorized administrator of Lehigh Preserve. For more information, please contact [preserve@lehigh.edu](mailto:preserve@lehigh.edu).

**FATIGUE TESTS OF  
WELDED PLATE GIRDERS IN BENDING**

by  
**Joseph A. Corrado**

**A Thesis**  
**Presented to the Graduate Faculty**  
**of Lehigh University**  
**in Candidacy for the Degree of**  
**Master of Science**

**Lehigh University**

**1965**

CERTIFICATE OF APPROVAL

This thesis is accepted and approved in partial fulfillment of the requirements for the degree of Master of Science in Civil Engineering.

May 20, 1965  
(Date)

Bung-Tsung Yen  
Professor Bung-Tsung Yen  
Professor in Charge

C. J. Hulsbos for  
Professor William J. Eney, Head  
Department of Civil Engineering

### ACKNOWLEDGMENTS

The experimental work which leads to this thesis is sponsored by the Pennsylvania Department of Highways in conjunction with the United States Department of Commerce-Bureau of Public Roads and the American Iron and Steel Institute through the Welding Research Council. All testing was performed at Fritz Engineering Laboratory, Department of Civil Engineering, Lehigh University, Bethlehem, Pennsylvania. Professor Lynn S. Beedle is Director of the Laboratory and Professor William J. Eney is Head of the Department. The sponsorship of the organizations and the general guidance of the professors are acknowledged.

The author is indebted to Mr. B. T. Yen for his guidance and advice on this thesis. The help that Mr. John A. Mueller provided in familiarizing the author with the fundamentals of the investigation and also his review of the manuscript is sincerely appreciated. Appreciation is extended to Messrs. Peter B. Cooper, Michael A. D'Apice, David J. Fielding and Hai-Sang Lew who assisted in conducting the tests. Assistance provided by Mr. Kyle Dudley in preparing the figures is gratefully acknowledged.

The assistance extended by the author's associates in Fritz Laboratory, particularly the shop personnel, supervised by Mr. Kenneth Harpel, shop foreman, is gratefully acknowledged. Appreciation is also extended to Mr. Heriberto Izquierdo for the drafting of the figures. The author expresses his sincere gratitude to Mrs. Dorothy Fielding for the typing of the manuscript.

TABLE OF CONTENTS

	<u>Page</u>
ABSTRACT	1
I. INTRODUCTION	2
II. DETAILS OF TEST SPECIMENS AND SETUP	4
2.1 Design Considerations and Description of Specimens	4
2.2 Properties and Characteristic Loads of Test Specimens	5
2.3 Test Setup and Instrumentation	6
A. Test Setup	6
B. Instrumentation	7
III. TESTING OF SPECIMENS	9
3.1 General Test Procedure	9
3.2 Testing of Girder F6	10
3.3 Testing of Girder F7	12
IV. TEST RESULTS	14
4.1 Fatigue Cracks	14
4.2 Lateral Web Deflections	15
A. Cross-Sectional Shapes of the Web	15
B. Web Deflection Contours	17
4.3 Web Stresses	18
V. DISCUSSION OF RESULTS	20
5.1 Cause of Primary Cracks	20
A. Lateral Web Deflections	20
B. Web Stresses	21
5.2 Comparison of Plate Girders and Beams in Bending	23

TABLE OF CONTENTS (continued)

	<u>Page</u>
VI. SUMMARY AND CONCLUSIONS	24
NOMENCLATURE	26
TABLES	27
FIGURES	31
REFERENCES	50
VITA	51

LIST OF TABLES

<u>Table</u>		<u>Page</u>
1	WELDING DETAILS	27
2	NOMINAL DIMENSIONS OF COMPONENT PARTS	28
3	PROPERTIES OF GIRDER COMPONENTS	28
4	GEOMETRIC PROPERTIES	29
5	CHARACTERISTIC LOADS	29
6	SUMMARY OF CRACK DATA	30



LIST OF FIGURES

<u>Figure</u>		<u>Page</u>
1	Test Specimen and Setup with Shear and Bending Moment Diagrams	31
2	Test Panels and Coordinate System	32
3	Overall View of Test Setup	32
4	Instrumentation	33
5	Static Load Versus Deflection, Girder F6	34
6	Fatigue Testing of Girder F6	35
7	Static Load Versus Deflection, Girder F7	36
8	Fatigue Testing of Girder F7	37
9	Web Cross-Sectional Shapes, Girder F7	38
10	Web Cross-Sectional Shapes, Girder F6	39
11	Web Deflection Contours, Girder F7	40
12	Web Deflection Contours, Girder F6	41
13	Components of Surface Stress	42
14	Web Stresses Normal to the Boundary, Girder F7	43
15	Web Stresses Normal to the Boundary, Girder F6	44
16	Cross-Sectional Distribution of Web Membrane Stresses, Girder F6	45
17	Cross-Sectional Distribution of Web Membrane Stresses, Girder F7	46
18	Typical Web Deflection	47
19	Approximate Cantilever Strip	48
20	Approximate Web Stresses Normal to the Boundary, Girder F6	49



ABSTRACT

This thesis describes fatigue tests of two welded plate girders subjected to pure bending. The purpose of the tests was to examine the fatigue behavior of slender webs in plate girders and to determine whether or not large lateral web deflections have any affect on the fatigue life of such members.

From an analysis of the test results, it is concluded that, in general, large lateral web deflections have little effect on the fatigue life of plate girders in bending. The fatigue behavior of plate girders in bending can be considered to be similar to that of beams subjected to repeated bending moments, and thus possibly can be designed accordingly for fatigue.

## I. INTRODUCTION

Up until about four years ago the design of the webs of plate girders to be used in buildings was based on the critical stress which would cause buckling of the web plate. Although this was the basis for design, the post-buckling strength of the web was implicitly recognized in practice by making use of a low factor of safety in the design of such members. In 1961, as a result of considerable theoretical and experimental research, (1,2,3,4) which clearly indicated the significance of the post-buckling strength of girders, the AISC adopted a specification for the design of plate girders which is based on the load carrying capacity of such members. Through this new provision, the use of slender webs is permitted thus making it possible to concentrate relatively more of the plate girder's material in the flanges. This becomes particularly advantageous for plate girders loaded primarily in bending.

This research which led to the code change was, in all cases, limited to investigations on the static load carrying behavior of plate girders. It is, then, logical to carry the research further, into the realm of repeated loading, in order to determine whether or not the large lateral web deflections which occur at high loads are significant in the life of plate girder members used in bridges. Also, it is particularly important to examine the behavior of very slender webs in plate girders subjected to repeated loads. These are a few of the reasons which have led to the fatigue tests of welded plate girders now being conducted at

Lehigh University. One phase of the experimentation deals with girders having slender webs and subjected to pure bending. In the following sections a discussion on this phase of the investigation is presented.

## II. DETAILS OF TEST SPECIMENS AND SETUP

### 2.1 Design Considerations and Description of Specimens

The design of the two specimens for these bending tests was based on a number of requirements. It was first necessary to have high maximum applied loads so that relatively large lateral deflections of the web would occur. Selection of the maximum load was influenced by the maximum capacity of the available loading jacks and pulsator. Also, it was essential that a load range be chosen such that the deflection of the girders between the maximum and minimum loads did not exceed the stroke limitation of the test setup which was about four-tenths of an inch.

For comparison purposes, it was desirable to design the specimens so that they would conform to previously tested plate girders.<sup>(4,5)</sup> Such considerations influenced the choice of the material (ASTM A373), the web depth and thickness of the test panels (50" x 3/16"), and the percentage of the static load-carrying capacity to be used as the maximum applied load (65%).

The configuration and geometry of the test girders resulting from the previous design considerations are shown in Fig. 1, together with the loading scheme, shear diagram, and bending moment diagram. The two girders were identical and were designated F6 and F7. The total length of each specimen measured 31 feet, of which the middle half was subjected to pure bending. That was the test section which consisted of three equal

50" test panels each having an aspect ratio of panel length to web depth ( $\alpha$ ) of 1.0 and numbered as indicated in Fig. 2. Test panels were separated by transverse stiffeners welded to each side of the web. These stiffeners were not connected to the tension flange so as to reduce the possibility of the formation of fatigue cracks in the flange. Web thickness for the test panels was 3/16", with a nominal web slenderness ratio of depth to thickness ( $\beta$ ) equal to 267. In order to limit the deflection of the girders, thicker (5/16") webs were used for the end sections as compared to the 3/16" plate in the middle.

For reference, the welding sequence and weld sizes, as provided by the fabricator, are given in Table 1, whereas the nominal dimensions of the girders' component parts are listed in Table 2.

## 2.2 Properties and Characteristic Loads of Test Girders

Actual dimensions of the component parts were obtained by taking measurements of representative samples cut from the original plates. Values that were obtained are listed in Table 3. Also listed in this table are the results of a chemical analysis of the steel (performed by the fabricator) and the physical properties (evaluated by the investigator by means of 8" standard coupon tests). It should be noted that the yield stress ( $\sigma_y$ ) was obtained under a zero strain rate and is referred to as the static yield stress. For the flanges, this stress was 32.6 ksi for girder F6 and 31.0 ksi for F7; for the 3/16" web of the test section it was 39.7 ksi for both specimens.

Calculation of the geometric properties of the girders was made using the measured dimensions. Tabulation of the aspect ratio ( $\alpha$ ), web

slenderness ratio ( $\beta$ ), web area ( $A_w$ ), moment of inertia (I), and section modulus (S) is made in Table 4.

With the dimensions and properties of the girders known, it was a simple matter to estimate the static load-carrying capacity. The ultimate load ( $P_u$ ) of the test section for F6 and F7 was calculated using ultimate strength theory<sup>(1)</sup> and was found to be 144 and 139 kips, respectively. Taking 65% of these ultimate loads, the maximum applied loads were evaluated to be 94 kips for F6 and 90 kips for F7. To serve as reference values the theoretical web buckling loads were calculated according to conventional practice.<sup>(4)</sup> Values of these and the previously mentioned loads are listed in Table 5.

### 2.3 Test Setup and Instrumentation

#### A. Test Setup

The specimens were tested on the dynamic test bed at the Fritz Engineering Laboratory of the Civil Engineering Department, Lehigh University. Supporting fixtures for the specimens simulated the end conditions for a simply-supported member. A two-point loading system was employed to provide the pure bending moment region for the test section (Fig. 1). Loading of the girders was furnished by two hydraulic jacks and two Amsler pulsators which were synchronized to provide a maximum load of 110 kips per jack at a frequency of about 250 cycles per minute.

In order to prevent the girder from moving out of the plane of loading, lateral supports were used at the two loading points in the form of 2-1/2" pipes. The pipes were pin-connected to the tops of the bearing stiffeners at one end and to structural support columns at the other. An overall view of the actual test setup can be seen in Fig. 3.

### B. Instrumentation

A Cartesian system of coordinates was adopted so that location of any point on a specimen would be possible. The system had its origin at the intersection of the girder's horizontal and vertical axes of symmetry as indicated in Fig. 2. Positive x and y values were measured to the right and upward, respectively. The z-axis, being perpendicular to the x-y plane, had its positive values measured in the direction of the near side of the specimen.

In order to study the behavior of the web plate, lateral web deflections were measured at various points of each test panel as indicated in Fig. 4a. These measurements were made using ten one-thousandth inch Ames dials fixed in position on a rigid, supporting frame. Reference values measured on a plane, finished surface were taken at regular intervals so as to compare them with the actual web readings. In this way, movement of the web out of its plane could easily be determined.

Electrical resistance strain gages were mounted in pairs on the web surfaces (near side and far side) of the test panels so that web stresses could be calculated. Gages were placed as close to the web boundaries as possible ( $3/4$  of an inch) in hope of obtaining an indication of the stress condition at the boundary. Most of the gages were mounted in a direction so as to measure strains perpendicular to the boundaries. Along the compression flange, strains were also measured parallel to the boundary. The orientation and locations of gages for girder F6 is shown in Fig. 4b. After 1,000,000 cycles of testing, twenty-four additional gages were added to measure strains in the tension zone of the web. Gages for girder F7 were mounted as indicated in Fig. 4c.

General behavior of the specimen was observed by recording the vertical deflections either under the load or at midspan by means of a one-thousandth inch Ames dial. Engineering level readings were taken at the supports and load points so that the elastic deflections could be checked.

During the fatigue testing of the specimens, visual inspections were made at regular two hour intervals to detect and examine fatigue cracks. Inspections were carried out with the aid of a three-power magnifying glass and a floodlight. Whitewashing of the specimens, prior to the time of testing, also aided in the inspection of fatigue cracks.



### III. TESTING OF SPECIMENS

#### 3.1 General Test Procedure

With a girder secured in the test bed, it was loaded slowly to the predetermined maximum load so as to check the test setup and the alignment. When that was satisfactory a complete set of readings for web deflections, strains, and girder deflections was taken at zero load. Static loading of the specimen to maximum load then followed with complete sets of readings being taken at various load magnitudes. Such load magnitudes were assigned sequential load numbers to facilitate the identification of test data.

Fatigue loading of the girder began after the static test. At a load range of practically zero to maximum, testing continued on a 24 hour basis until it was necessary either to effect a repair or to terminate the test. Throughout the fatigue test, visual inspection of all welds was made at regular two hour periods (31,500 cycles).

Whenever a crack was discovered, it was marked and its growth observed and measured at every inspection. When necessary, testing was temporarily stopped for repair of the cracks. In some instances, after the repair, complete sets of readings were taken at the various static load levels to check the effects of the repair, if any, on the web's strains and lateral deflections. Following this, fatigue testing was resumed and the sequence of testing and repairing was carried on until the termination of the test.

Detailed discussions of the actual tests of the two specimens are presented in the following sections.

### 3.2 Testing of Girder F6

For the static test of girder F6, sets of readings were taken at 5, 15, 30, 47, 60, 75 and 94 kips, the latter being the maximum value for fatigue loading. As can be seen in the plot of static load versus girder deflection (Fig. 5), the general behavior of the specimen, in terms of girder deflection, was in good agreement with that predicted theoretically.

Fatigue testing proceeded at a measured rate of 262.5 load cycles per minute from 5 to 94 kips. At 600,000 cycles a pair of cracks, referred to as Cracks 1 and 2, were found on the far side of the web in test panel 1. Both cracks had initiated at the web-stiffener boundaries in the web, at the toe of the weld, and propagated parallel to the stiffener. After a total of 693,000 cycles, cracks were observed outside the test section in the web butt welds at  $x = \pm 82\frac{1}{2}$ . At 756,000 cycles it was decided that a repair would be made before relatively serious damage had been imposed by the butt-weld cracks. At that moment inspection revealed that Cracks 1 and 2 had propagated through the thickness of the web and had total lengths of 14 and 10 inches, respectively. (Close observation of Crack 2 indicated that it had not penetrated into the tension flange.) Final appearance and location of these cracks are shown in Fig. 6a. The history of loading is diagrammatically presented in Fig. 6b.

All cracks were repaired by first gouging out the fractured material with an air hammer chisel or grinding stone, or both, and then filling the cavity with weld material. In addition, panel 1 was stiffened

by welding two 5" x 5/16" plates to the far side of the web at the panel's one-third points, as shown in Fig. 6a. This overall repair of all cracks is indicated in Fig. 6b as Repairs 1 and 2.

When testing was resumed, the cracks at the butt welds reappeared almost immediately. At a total of 869,000 cycles a crack appeared at the location of the repaired Crack 2 (referred to as Crack 2a). At 1,000,000 cycles testing was stopped for a careful inspection of all cracks. Plug samples were cut from the web butt welds adjacent to the flanges. When incomplete penetration of the welds was observed, the butt welds were completely removed and replaced. The voids which resulted from the inspection remained as cope holes. Along with these repairs (Repair A, Fig. 6b), an attempt was made to repair Crack 2a by gouging and welding.

Because of the excessive repairs a static test was performed before cyclic loading was resumed. Not long after pulsating was underway once again, Crack 2b appeared at the repair weld of Crack 2a at a total of 1,040,000 cycles. This crack was repaired shortly thereafter by first gouging and welding; then partially cutting away the intermediate stiffener and welding 8" x 20" x 5/16" doubler plates to the web at the location of the crack, as indicated in Fig. 6a.

Crack 3 was first observed along a stiffener (Fig. 6a) at 1,242,450 cycles. Before a repair was effected at 1,300,000 cycles this crack had grown to a total length of 5 inches. Repair (Repair 3) was made by first cutting away a small section of the stiffener, then gouging out the fractured material and welding.

Upon continuation of the test, cracks formed adjacent to the cope holes at the web butt welds. Another crack appeared at 1,372,000 cycles at the bottom of the tension flange, directly below the original Crack 2 and possibly an outgrowth of the same crack. Due to these cracks the stiffness of the girder began to decrease slightly as indicated by a measurable drop in the maximum load and an increase in the girder's deflection. Further repairs of the girder would not have significantly increased its life; therefore, the test was terminated at a total of 1,376,000 cycles.

### 3.3 Testing of Girder F7

Except for the load magnitudes, the procedure for the static test of girder F7 was identical to that for girder F6. Strain and deflection readings were taken at loads of 0, 5, 15, 30, 38, 45, 60, and 76 kips. The maximum load was decreased from the intended 90 kips to 76 kips in an attempt to eliminate the formation of cracks at the butt welds. The plot in Fig. 7 indicates that, similar to F6, the specimen behaved statically in a manner predicted by conventional theory.

At 1,252,000 cycles after the beginning of fatigue testing, a crack was observed in the butt weld at  $x = - 82\frac{1}{2}$ . Following this observation, testing was stopped at 1,300,000 cycles and inspection of the butt welds made by once again cutting plug samples from the welds. A complete repair, identical to that for girder F6, was found necessary for the butt welds.

When this repair (Repair A, Fig. 8) was completed a static test was run prior to the continuation of the fatigue test. At this time the

maximum load was reset to 90 kips so that a more direct comparison of the test results for the two specimens would be possible.

With a load range of 5 to 90 kips, fatigue testing continued for 980,000 cycles (2,280,000 total cycles) before a crack was observed to form in the test section. The crack (Crack 1, Fig. 8a) was found along the lower part of the stiffener in test panel 3. It grew in length to about 4 inches before a repair was made at 2,330,000 cycles. Thereafter no cracks were detected in the test section. Due to cracks which appeared at the cope holes, testing was terminated at a total of 2,879,000 cycles.

#### IV. TEST RESULTS

In reviewing the history of the girder tests, results were given only in regard to the number of cycles at which fatigue cracks were first observed. The details of all these cracks are summarized in the next section, followed by the presentation of the results on web deflections and stresses.

##### 4.1 Fatigue Cracks

Fatigue cracks that occurred during the tests are arbitrarily divided into "primary cracks", which formed in the test section, and cracks which appeared at the butt welds and cope holes.

In table 6 are listed the reference coordinates of each primary crack at first observation, the corresponding total number of cycles, and the final length of the cracks at repair. All these cracks initiated in the web at the toe of the stiffener fillet weld. The cracks always formed in the tension zone of the web and propagated in a direction parallel to the boundary. Cracks 1 and 2 of girder F6 appeared only on the far side (-z) of the web when first observed, whereas the other cracks could be seen from both sides.

Cracks at the butt welds and cope holes were found in both the tension and compression regions of the web, close to the flanges. A study of these cracks is in the realm of structural details and is not

within the domain of this investigation. It seems sufficient to point out that the occurrence of these cracks might have been strongly influenced by the incomplete penetration of the butt welds.

One significant observation was the result of repairing the cracks. Both Cracks 1 and 2 of girder F6 were subjected to the identical treatment of removing the fractured material, depositing of weld material, and stiffening of the panel. Yet Crack 1 was successfully eliminated, but Crack 2 reappeared immediately. The cause of such a difference will be discussed later.

There was another group of cracks which were detected following the termination of the test for girder F7. These were three very fine, vertical, hair cracks in the fillet weld at the web-to-compression flange boundary in the test section. Such cracks possibly could have been due to the presence of residual stresses. Cracks of similar nature have been observed in previous tests and were found to have an insignificant effect on the test results. (5)

#### 4.2 Lateral Web Deflections

Cross-sectional shapes and contours of the laterally deflected web were prepared for selected load magnitudes in order that the out-of-plane movement of the web could be visualized. The data used in preparing these plots were obtained from the static test measurements.

##### A. Cross-sectional Shapes of the Web

For a description of the web cross-sectional shapes, reference is made to those for girder F7, Fig. 9. An outline sketch of the test section is shown together with the x and y coordinates. The shapes for loads of

zero, half-maximum, and maximum were approximated by connecting with straight lines the measured lateral deflections at given web points. Deflections ( $w$ ) in the positive  $z$ -direction (near side deflections) are plotted to the right of the vertical line, whereas those in the negative  $z$ -direction (far side deflections) are plotted to the left.

From Fig. 9, it can be seen that large relative lateral deflections between zero and maximum load occurred in the compression zone of the web, while the corresponding deflections in the tension zone were quite small. Deflection patterns of this type can be considered to be a common occurrence for girders in bending as evidenced by results of these and previous tests. <sup>(4)</sup> The magnitudes of the relative deflections (from 0 to 90 kips) in the compression zone of F7 were in the order of the web's thickness (3/16").

The deflected shape for panel 1, girder F6, differed from the common case in that large relative web deflections between the test loads occurred not only in the compression zone, but also in the tension zone (Fig. 10). The magnitudes of these movements were about 2-1/2 times the web's thickness for the compression zone and approximately equal to the web's thickness for the tension zone. Even at only a short distance (6-1/2") away from a stiffener ( $x = -75$ ), the relative deflections were found to be unusually large below the girder's neutral axis. The reason for such unusually large movements for this panel is the shifting of the deflected position of the web from one side of the vertical to the other during loading. This shifting movement did not take place for the other two test panels of girder F6, nor did it take place in any of the panels of girder F7 (Fig. 9).



### B. Web Deflection Contours

In order that a more complete picture of the deflected web would be available for examination, web deflection contours are presented in Figs. 11 and 12 for a test panel for each girder. In these figures a contour interval of 0.03 inch is adopted, with the near side deflections being indicated by the solid lines and the far side movements shown by the broken lines. Contours for zero, half-maximum, and maximum load are given for each panel.

A review of Fig. 11 indicates that the upper portion of panel 3, girder F7 was far from being plane at zero load. As the load was increased, deflections changed gradually and practically maintained the same pattern. By the decreasing of contour lines in the lower part of the panel, it is evident that the web was being straightened as load was applied. In the area where Crack 1 formed, there was little deflection of the web.

From the deflection contours for panel 1, girder F6 (Fig. 12), the shifting movement of the web from one side to the other can clearly be observed. After the shifting between zero and 47 kips, the pattern of deflection was consistent, with only changes in the magnitude of deflection. Contrary to the common pattern of Fig. 11, intense contour lines appeared in the lower region of the panel, thus indicating relatively large web deflection in the tension zone. All these imply serious web movement, even near the boundary, and was observed so during testing. However, in the vicinity of Crack 2, the web almost remained stationary.

#### 4.3 Web Stresses

Stresses that were directly calculated from the strain gage measurements were those which existed on the surface of the web, and are referred to as surface stresses. Surface stresses that were perpendicular to the web-stiffener boundaries were calculated as the product of the measured strain ( $\epsilon$ ) and the modulus of elasticity ( $E = 29.6 \times 10^3$  ksi). For similar stresses normal to the web-flange boundaries, the Poisson effect was taken into account.

By knowing the values of these surface stresses at various points on both the near and far side of the web, it was possible to decompose the surface stress into component parts, that is, into membrane and secondary bending stress. The membrane stress results primarily from bending of the girder in its plane, and is considered to be distributed uniformly across the thickness of the web. Secondary bending stress, also referred to as plate bending stress, is caused by the lateral movement of the web. This component of the surface stress has a linear distribution across the web's thickness as indicated in Fig. 13.

The surface, membrane, and secondary bending stresses normal to the web boundaries are given as vectors in Figs. 14 and 15 for girders F7 and F6, respectively, for their maximum applied loads. These stresses are for points  $3/4$  of an inch away from the face of the transverse stiffener or compression flange, whichever the case may be. An "F" adjacent to any of the stress vectors designates the stress value on the far side of the web, and values that were less than 2 ksi are indicated by a dot in these figures.

For the surface stresses (Figs. 14a and 15a), the larger tensile value for the two faces of the web was plotted. (If compressive values existed on both surfaces, then the smaller of these was used.) By the length of the stress vectors, it is seen that the surface stresses for both girders were highest in the upper portion of the web, perpendicular to the web-flange boundary (20 - 30 ksi). The component membrane stresses in Figs. 14b and 15b indicate that measured values were in good agreement with the theoretical values of  $\sigma = Mc/I$ , which are marked as a dash adjacent to the plotted measured values. Membrane stresses perpendicular to the compression flange were in all cases very small. In Figs. 14c and 15c the vectors for the secondary bending (plate bending) stresses were large (20 - 30 ksi) in the compression zone of the web, but significantly smaller in the tension zone. It is obvious that the component of secondary bending stress constitutes the main part of the surface stresses perpendicular to the compression flange.

The agreement between the measured membrane stresses and the theoretical values is depicted further by plotting in Figs. 16 and 17 the stress distributions at cross sections near the stiffeners. Slight deviation could possibly be attributed to the effect of lateral web deflections in the panels. In general the membrane tensile stresses below the neutral axis can be regarded as well represented by the theoretical values calculated from the flexural formula.

## V. DISCUSSION OF RESULTS

In the previous chapter the details of fatigue cracks, web deflections, and web stresses were presented. This chapter contains an examination of these results in an attempt to relate some consistent factor to crack initiation.

### 5.1 Cause of Primary Cracks

#### A. Lateral Web Deflections

The results from the web deflection measurements agreed very well with what was expected. Large lateral deflections occurred in the upper portion of the web, whereas below the girder's neutral axis the web deflections were small. This common deflected configuration for girders in bending is shown in Fig. 18. For fatigue loading between two load levels, the web fluctuates between two similar deflection configurations; thus the relative movement could also be closely approximated by the deflected shape in Fig. 18. If repeated relative web deflections were the sole cause of fatigue cracks in girders subjected to bending, cracks would form in the upper region of the web, parallel to the boundaries. However, this was not the case. Three of the four primary cracks (Cracks 2 and 3, F6 and Crack 1, F7) formed in the lower part of the web where there was little or no web deflection. Only the fourth primary crack (Crack 1 of F6) formed in a section of the web which had noticeable lateral deflection, but was below the neutral axis of the girder, not above. The success of the repair

of this crack, which effectively reduced the deflections in the panel to zero, lends credence to the belief that this crack was at least partly due to lateral web deflections. Similar, successful repairs of cracks in previous test girders with large web deflections substantiates the above. (5)

Since lateral web deflections cause stresses which, in turn, may affect the formation of fatigue cracks, an examination of these web stresses follows.

#### B. Web Stresses

It was previously pointed out that secondary (plate) bending stresses are due to lateral web movement. Therefore, large secondary bending stresses should accompany large lateral deflections. That this is true is indicated by the stress vectors in Fig. 14c, where large vectors are in the upper region and small vectors in the lower region.

Additional proof is provided by Fig. 15c for the compression zone of girder F6. Values of the plate bending stress at points below the neutral axis were not available prior to the formation of Cracks 1 and 2. However, after 1,000,000 cycles of load, these stresses were calculated to be in the order of 3 ksi for panels 2 and 3, where the web deflections were small. In order to obtain an evaluation of the plate bending stresses in the lower portion of panel 1 before the formation of cracks, it was necessary to use an approximate approach.

By considering an imaginary cantilever strip of unit width and using measured web deflections, as indicated in Fig. 19, a deflected shape of the web could be obtained in the form,

$$w = a x^5 + b x^4 + c x^3 + d x^2$$

From this, the secondary bending stresses were calculated at the toe of the fillet welds. These stresses are shown in Fig. 20 along with the approximate membrane ( $M_c/I$ ) and resulting surface stresses. The magnitudes of the plate bending stress for panel 1 were highest (25 - 35 ksi) in the upper part of the web, yet Crack 1 initiated about 9 inches below the neutral axis where the plate bending stress was about 20 ksi.

Since secondary bending stress is not necessarily the controlling factor, and since all the other primary cracks formed where there was little or no plate bending stress, an examination of the membrane stress in these areas is in order.

A review of the web membrane stresses, Figs. 16 and 17, reveals that at Cracks 2 and 3 of girder F6 and Crack 1 of girder F7 these stresses were about 16 ksi. Compared with the negligible secondary bending stress, it appears that the tensile membrane stress is dominant in the formation of fatigue cracks.

A further look at the stress picture in the vicinity of Crack 1, girder F6, indicates that the combination of secondary bending stress of about 20 ksi and tensile membrane stress of about 7 ksi resulted in a condition of stress which, most likely, was the cause of Crack 1. However, this condition does not seem to be the general case for bending girders, because large web deflections in the tension zone of the web are uncommon. Thus, in general, plate bending stress has little effect on the formation of fatigue cracks in plate girders subjected primarily to bending, whereas tensile membrane stresses have a dominant effect.

## 5.2 Comparison of Plate Girders and Beams in Bending

Because tensile membrane stresses - which can be predicted by beam theory - play a dominant role in crack formation, it seems logical to compare the fatigue behavior of girders with that of beams.

A considerable amount of research has been conducted on beams subjected to repeated bending moments. (6,7,8,9) Fatigue cracks usually initiated in the tension flange, along transverse stiffeners, at cope holes, at the ends of partial length cover plates, or at butt welds. Except for Crack 1, girder F6, which was partly due to lateral web deflection, all cracks in girders F6 and F7 are included in the failure modes associated with beams.

For beams with similar stiffener details as those for the test girders, numerous tests reveal that cracks form along stiffeners and cause "failure" at about 2,000,000 cycles for a stress range of essentially zero to 18 ksi. (Fig. 10.6, Ref. 7) For the test girders, Cracks 2 and 3 of girder F6 were "first observed" at 600,000 and 1,240,000 cycles, respectively, whereas Crack 1 of girder F7 was found at 2,280,000 cycles. All were subjected to a stress range of approximately zero to 16 ksi. The difference in these results can possibly be attributed to the scatter that occurs in fatigue testing, and the deviation from the results of the beam tests may partly be due to the fact that the definition of "failure" is not the same for the beam and girder tests. Additional data from girder tests should render further verification.

Based on this discussion, it is highly possible that plate girders subjected primarily to bending can be regarded as beams and thus can be designed accordingly for fatigue.

## VI. SUMMARY AND CONCLUSIONS

A summary of the test results from the experimental work described in this report follows:

1. Slender webs of plate girders fluctuate laterally under repeated high bending moments.
2. The lateral deflection of the web is more pronounced in the compression zone than in the tension portion of the girder. Consequently, the magnitude of fluctuation of the web is also larger in the compression zone.
3. High plate (secondary) bending stresses occur on the web's surfaces in areas where lateral web deflections are large.
4. All primary fatigue cracks formed below the neutral axis of the girder, in regions where the web deflections or plate bending stresses were not largest.
5. At the initiation point of all primary cracks tensile web membrane stresses were of appreciable magnitude.
6. Web membrane stresses in the tension zone of the web can be closely predicted from  $M_c/I$ .
7. In some instances a combination of tensile membrane and plate bending stresses may cause a fatigue crack to form.
8. Successful repair of fatigue cracks due to lateral web deflections is possible, as evidenced from these and previous tests.
9. In general, the modes of crack initiation in plate girders subjected primarily to bending are similar to those for beams.



From the results and discussions previously presented the following conclusions can be made for welded plate girders subjected to repeated bending loads:

1. In general, large lateral web deflections that occur at high loads have little effect on the fatigue life of plate girders subjected primarily to bending.
2. Tensile membrane stresses appear to be dominant in the formation of fatigue cracks.
3. It is highly probable that the fatigue behavior of plate girders in bending is similar to that of beams. Therefore, they possibly can be designed accordingly for fatigue.

NOMENCLATURE

a	panel length
b	web depth
t	web thickness
v	deflection in the y - direction
$v_p$	deflection in the y - direction at load point
w	deflection in the z - direction
x, y, z	Cartesian coordinate axes
$A_w$	web area
E	modulus of elasticity (29,600 ksi)
I	moment of inertia about horizontal centroidal axis
P	load applied by one hydraulic jack
$P_{cr}$	theoretical web buckling load
$P_{min.}$	minimum applied fatigue load
$P_{max.}$	maximum applied fatigue load
$P_u$	theoretically obtained static ultimate load
S	section modulus
$\alpha$	aspect ratio, a/b
$\beta$	web slenderness ratio, b/t
$\epsilon$	strain
$\epsilon_y$	yield strain
$\mu$	Poisson's ratio (0.3)
$\sigma$	stress
$\sigma_y$	yield stress
$\sigma_u$	ultimate tensile stress

TABLE 1 WELDING DETAILS

A. Sequence

Step	Connection	Position	Weld
1	5/16" Web Plates to Flanges	N. S.	a
	3/16" Web Plates to Flanges	N. S.	b
2	Bearing Stiff. to 5/16" Web Plates	N. S.	a
	Inter. Stiff. to 3/16" Web Plate	N. S.	b
3	5/16" Web Plates to 3/16" Web Plate	N. S.	c
4	Same as Step 1 above	F. S.	As above
5	Same as Step 2 above	F. S.	As above
6	Same as Step 3 above	F. S.	d

B. Welds

Weld	Type	Details	Remarks
a	1/4 fillet	co <sub>2</sub> , 200A, 22v, 10ipm	0.045" dia. wire, 50 cu. ft. per in. gas flow
b	1/8 fillet	co <sub>2</sub> , 200A, 22v, 20ipm	
c	Butt	co <sub>2</sub> , 200A, 22v, 20ipm	
d	Butt	co <sub>2</sub> , 350A, 27v, 18ipm	

TABLE 2 NOMINAL DIMENSIONS OF COMPONENT PARTS\*

Girder	Test Section			End Section		
	Flanges	Web	Stiffener Spacing	Flanges	Web	Stiffener Spacing
F6	12 x 5/8	50 x 3/16	50	12 x 5/8	50 x 5/16	90
F7	12 x 5/8	50 x 3/16	50	12 x 5/8	50 x 5/16	90

\*Dimensions in inches

TABLE 3 PROPERTIES OF GIRDER COMPONENTS

Girder Component		Dimensions (inches)	Chemical Properties					Physical Properties			
			C (%)	Mn (%)	P (%)	S (%)	Si (%)	$\sigma_y$ (ksi)	$\sigma_u$ (ksi)	Elong. (%)	
F6	Test	Flanges	12.13 x 0.628	0.22	0.57	0.009	0.017	0.05	32.6	62.7	29.5
		Web	50 x 0.182	0.15	0.51	0.008	0.019	0.04	39.7	59.0	28.3
	End	Flanges	12.13 x 0.628	0.22	0.57	0.009	0.017	0.05	32.6	62.7	29.5
		Web	50 x 0.312	0.15	0.51	0.008	0.019	0.04	35.2	58.6	30.5
F7	Test	Flanges	12.15 x 0.638	0.16	0.72	0.008	0.022	0.03	31.0	57.8	31.9
		Web	50 x 0.182	0.15	0.51	0.008	0.019	0.04	39.7	59.0	28.3
	End	Flanges	12.15 x 0.638	0.16	0.72	0.008	0.022	0.03	31.0	57.8	31.9
		Web	50 x 0.312	0.15	0.51	0.008	0.019	0.04	35.2	58.6	30.5

TABLE 4 GEOMETRIC PROPERTIES

Girder		$\alpha$	$\beta$	$A_w$ (in. <sup>2</sup> )	I (in. <sup>4</sup> )	S (in. <sup>3</sup> )
Test Section	F6	1.0	275	9.10	11,660	455.0
	F7	1.0	275	9.10	11,832	461.5
End Section	F6	1.8	160	15.60	13,020	508.0
	F7	1.8	160	15.60	13,190	514.5

TABLE 5 CHARACTERISTIC LOADS

Girder		$P_{cr}$ (kips)	$P_u$ (kips)	$P_{min.}$ (kips)	$P_{max.}$ (kips)	% $P_u$	
						$P_{min.}$	$P_{max.}$
Test Section	F6	43.8	144	5	94	3.5	65.3
	F7	44.4	139	5	76 90*	3.6	54.7 64.8*
End Section	F6	94.5	162	5	94	3.1	58.0
	F7	95.0	158	5	76 90*	3.2	48.1 57.0*

\*Test loads changed after 1,300,000 cycles

TABLE 6 SUMMARY OF CRACK DATA

Girder	Crack	First Observation			At Repair		
		Coordinates			Cycles	Total Cycles	Length (in.)
		x	y	z			
F6	1	$-74 \frac{3}{4}$	- 8 , -10	$-3/32$	600,200	756,000	14
	2	$-25 \frac{1}{4}$	$-20 \frac{1}{2}$ , $-22 \frac{1}{2}$	$-3/32$	600,200	756,000	10
	3	$+24 \frac{7}{8}$	$-20 \frac{1}{2}$ , $-23 \frac{1}{2}$	$\pm 3/32$	1,242,450	1,300,000	5
F7	1	$+74 \frac{1}{2}$	$-22 \frac{1}{4}$ , -24	$\pm 3/32$	2,280,650	2,330,000	4



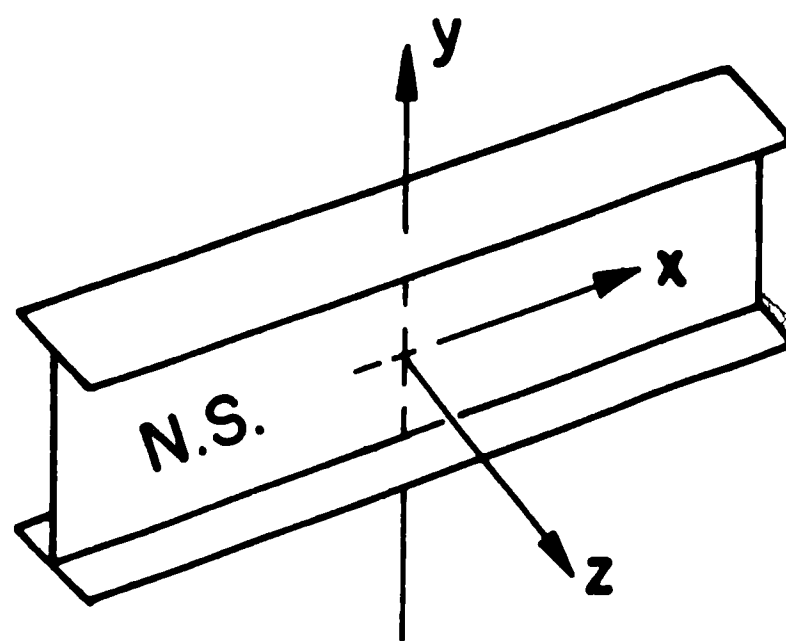
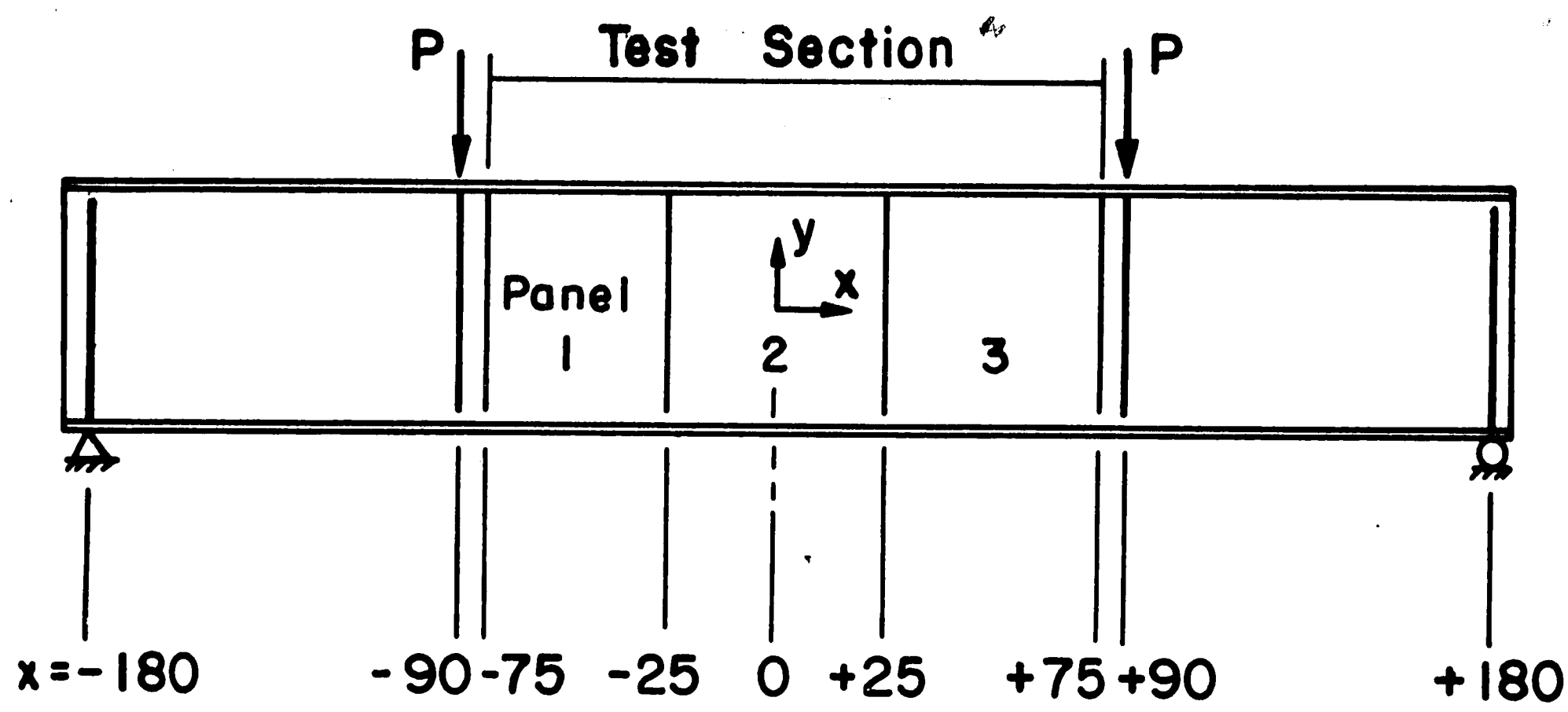


Fig. 2 Test Panels and Coordinate System

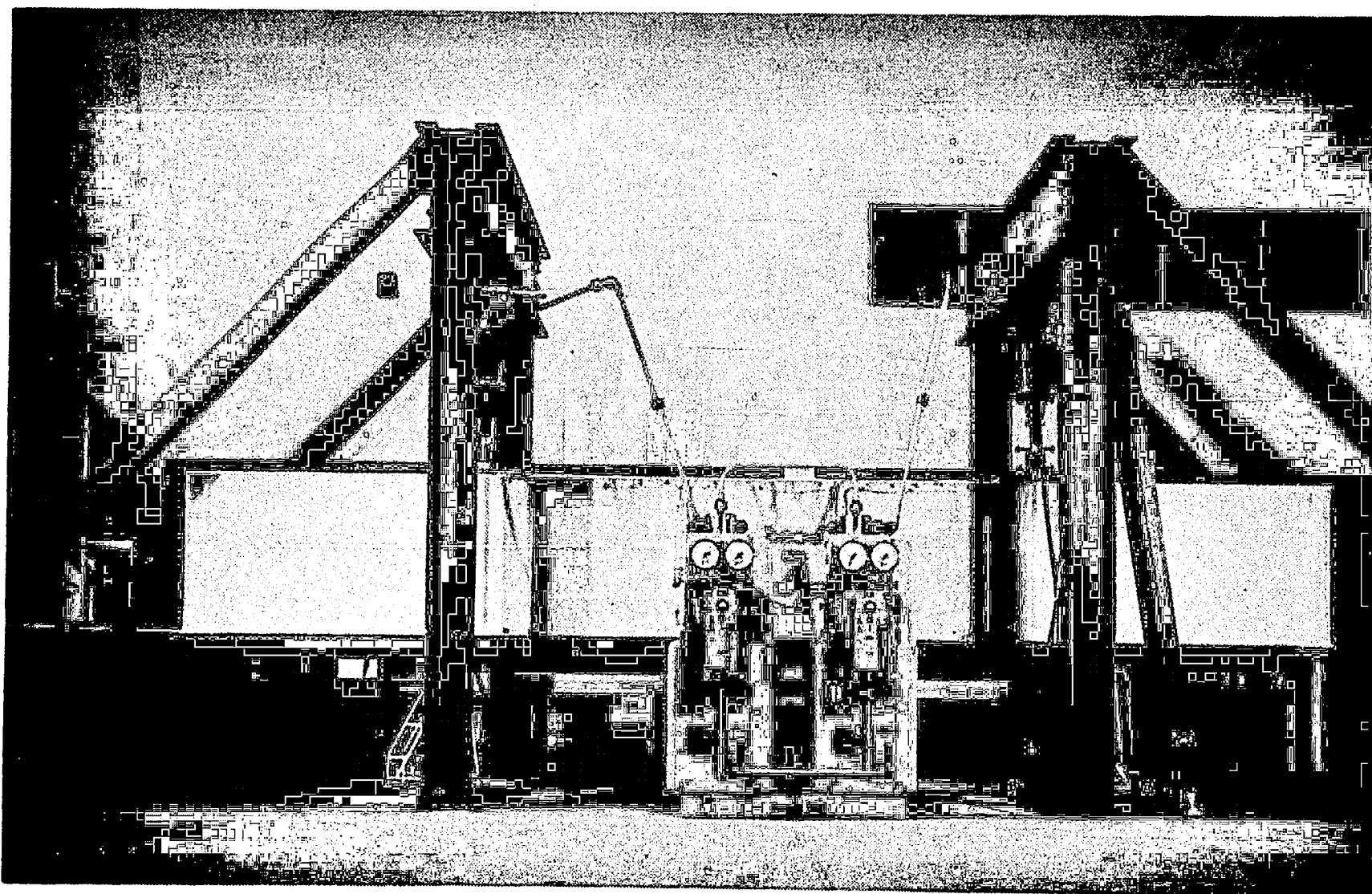
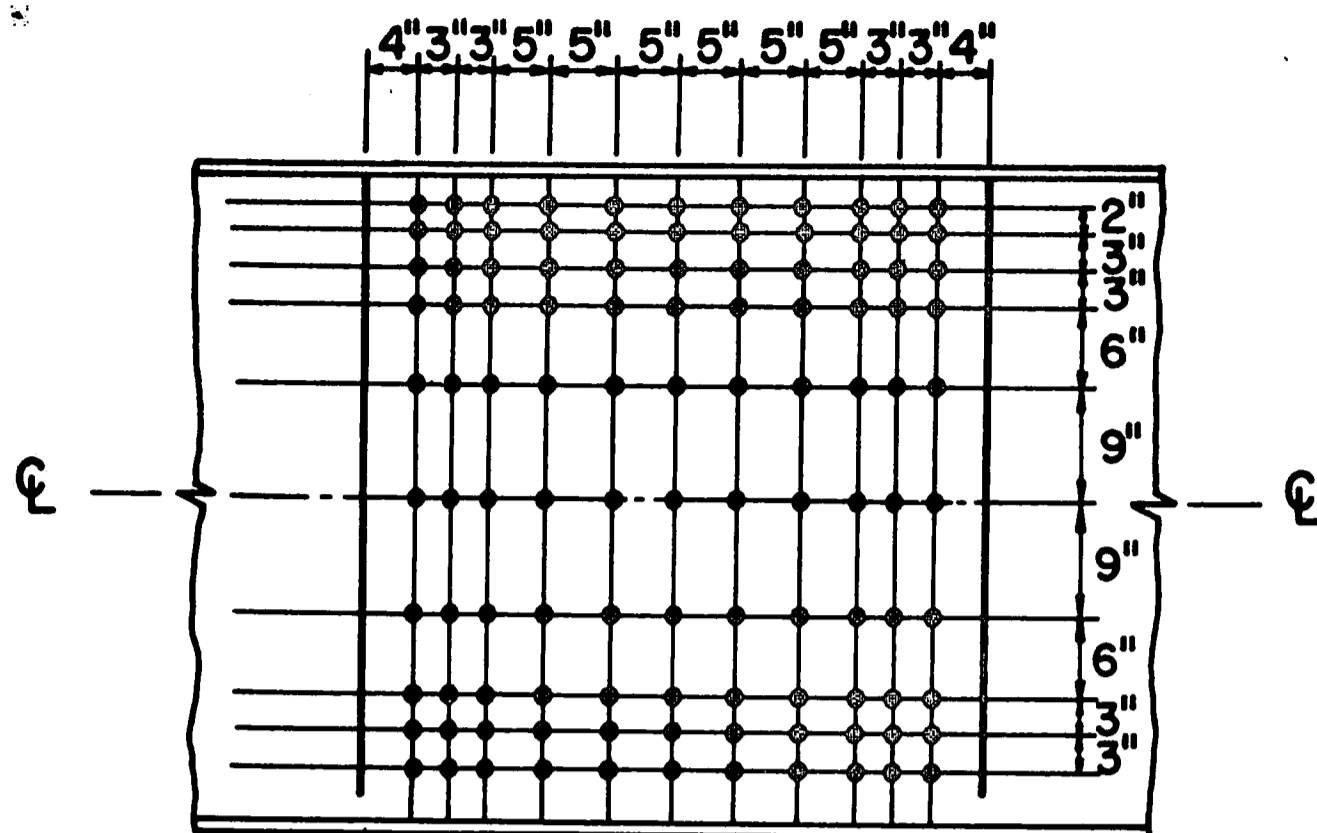
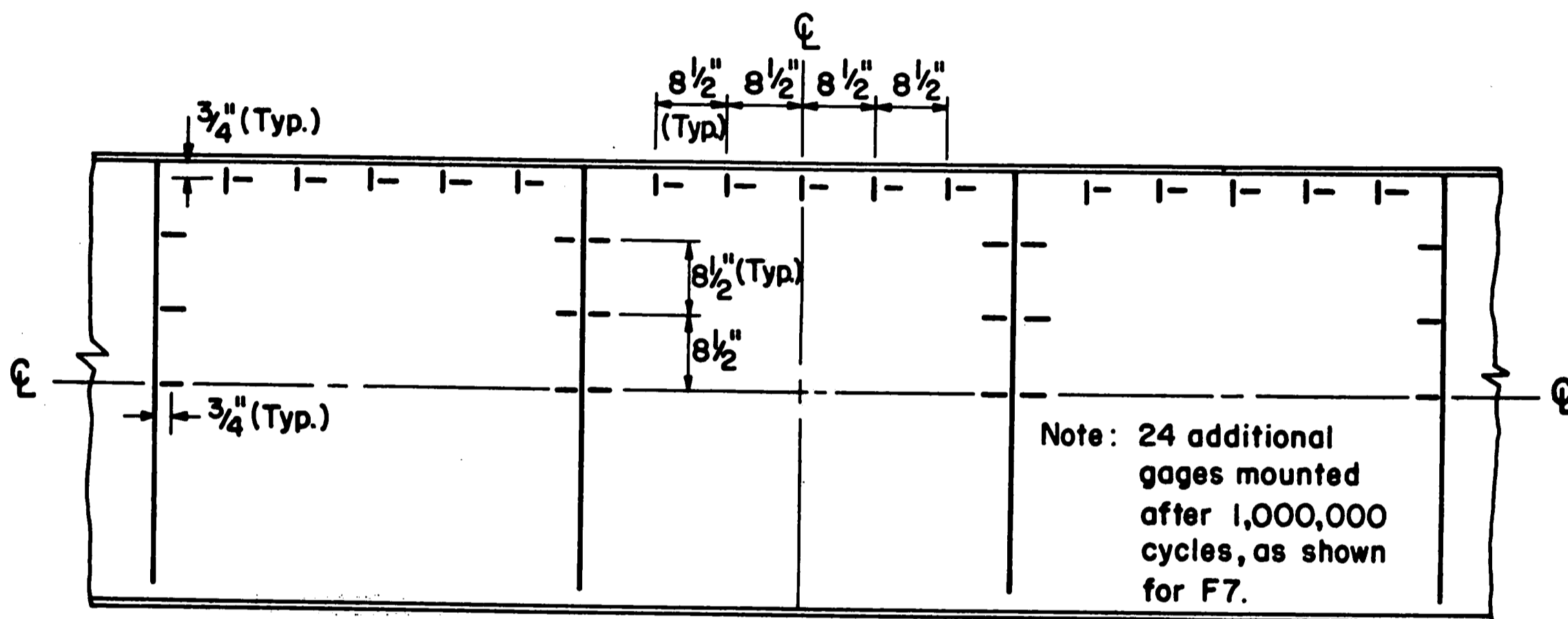


Fig. 3 Overall View of Test Setup

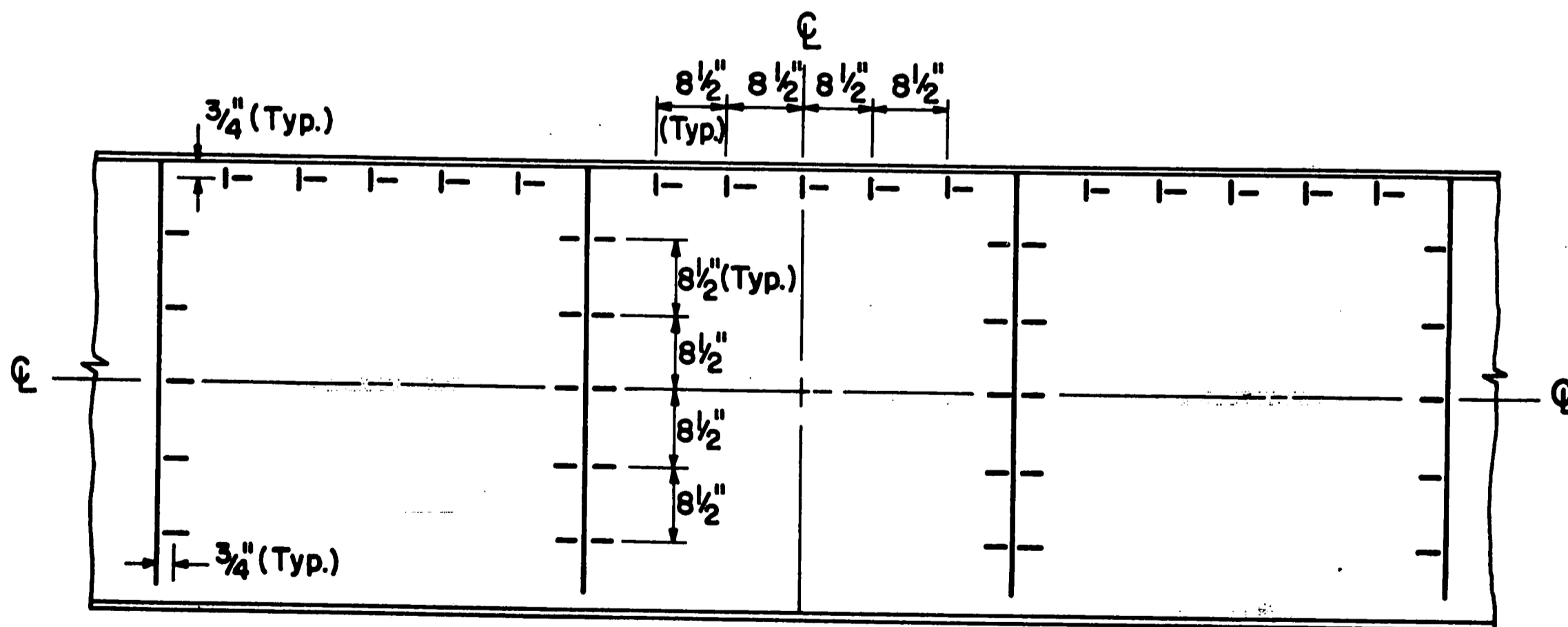




(a) Locations of Lateral Web Deflection Measurements (Typ.)



(b) SR4-A1 Gages, Girder F6



(c) SR4-A1 Gages, Girder F7

Fig. 4 Instrumentation

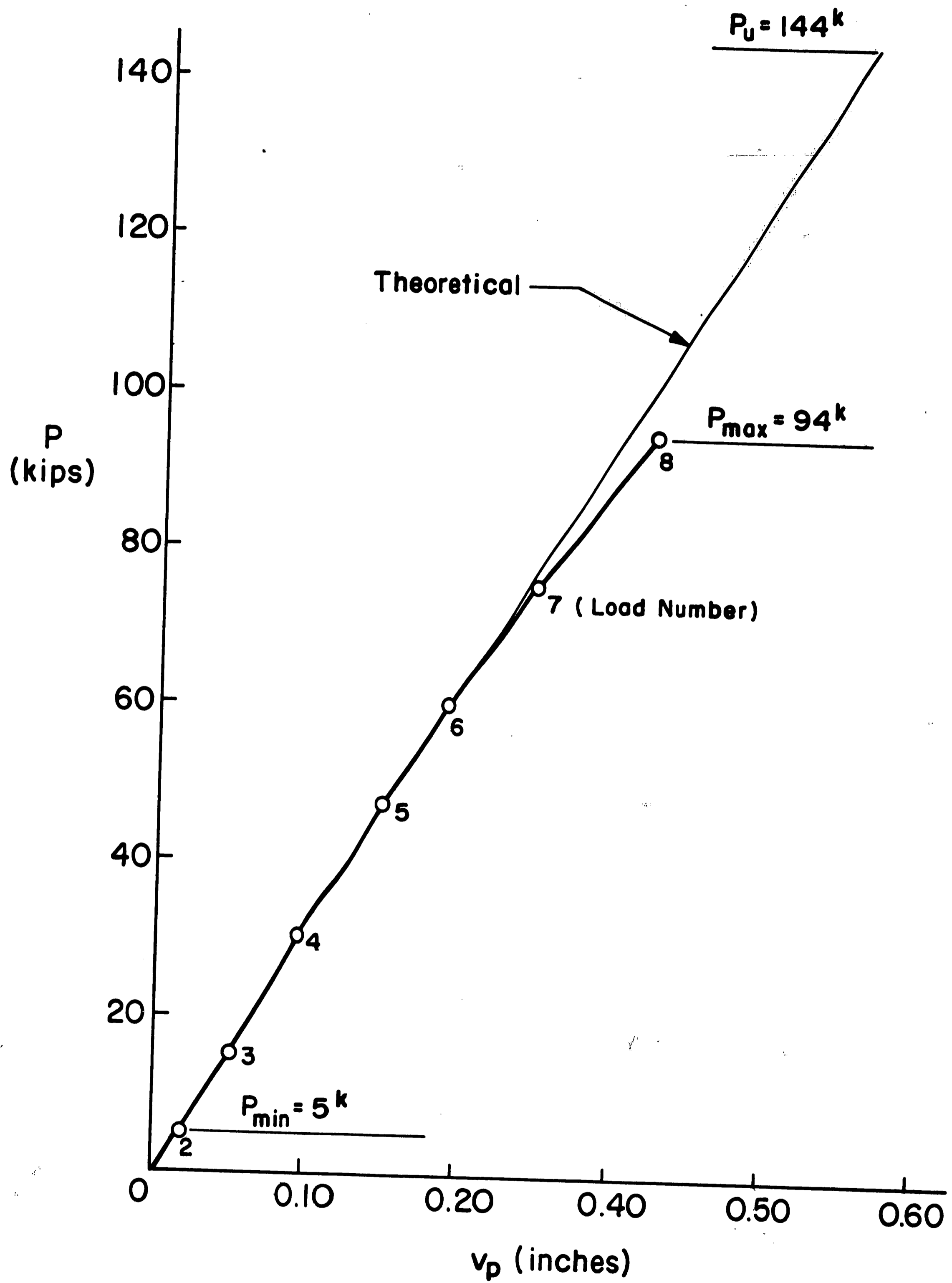
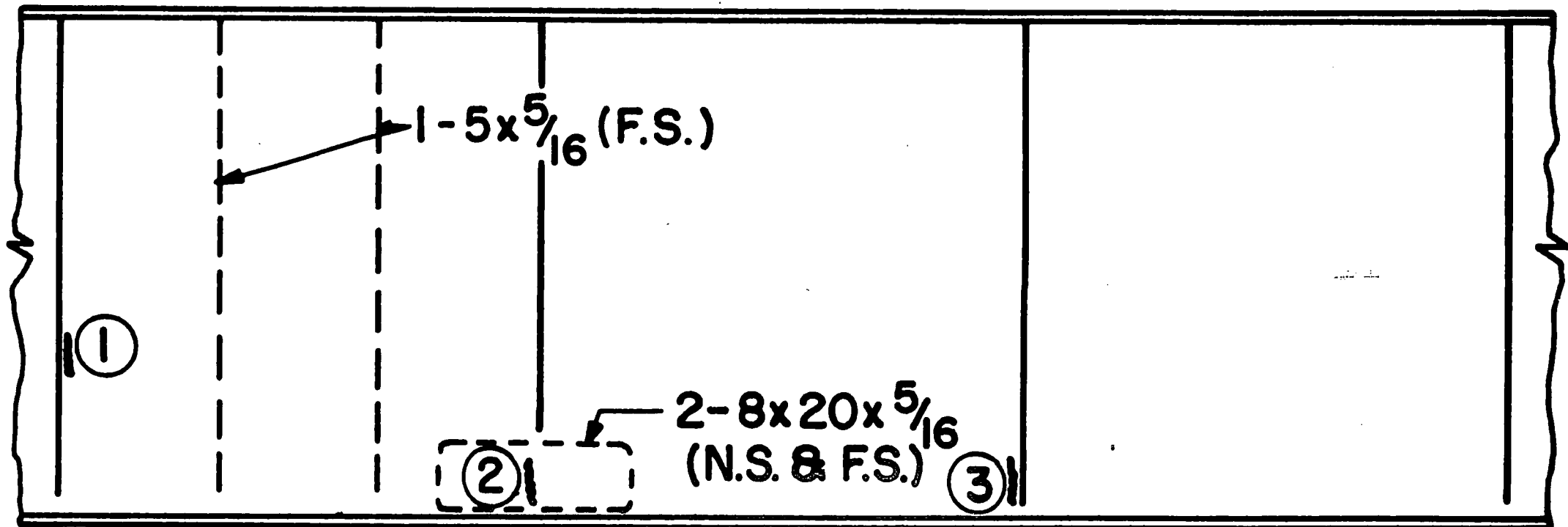
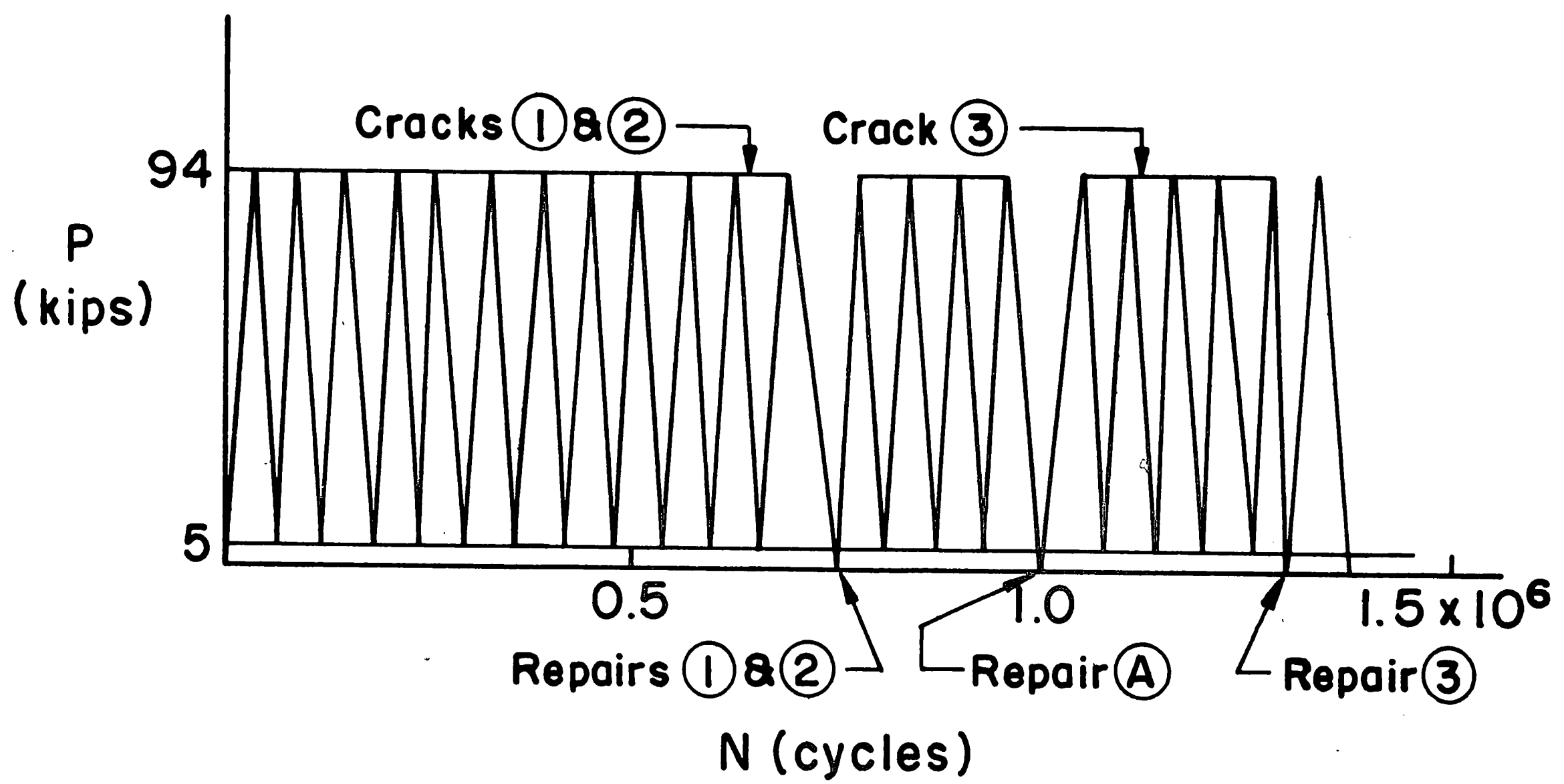


Fig. 5 Static Load Versus Deflection, Girder F6



(a) Crack Location and Repair



(b) Fatigue Test Sequence

Fig. 6 Fatigue Testing of Girder F6

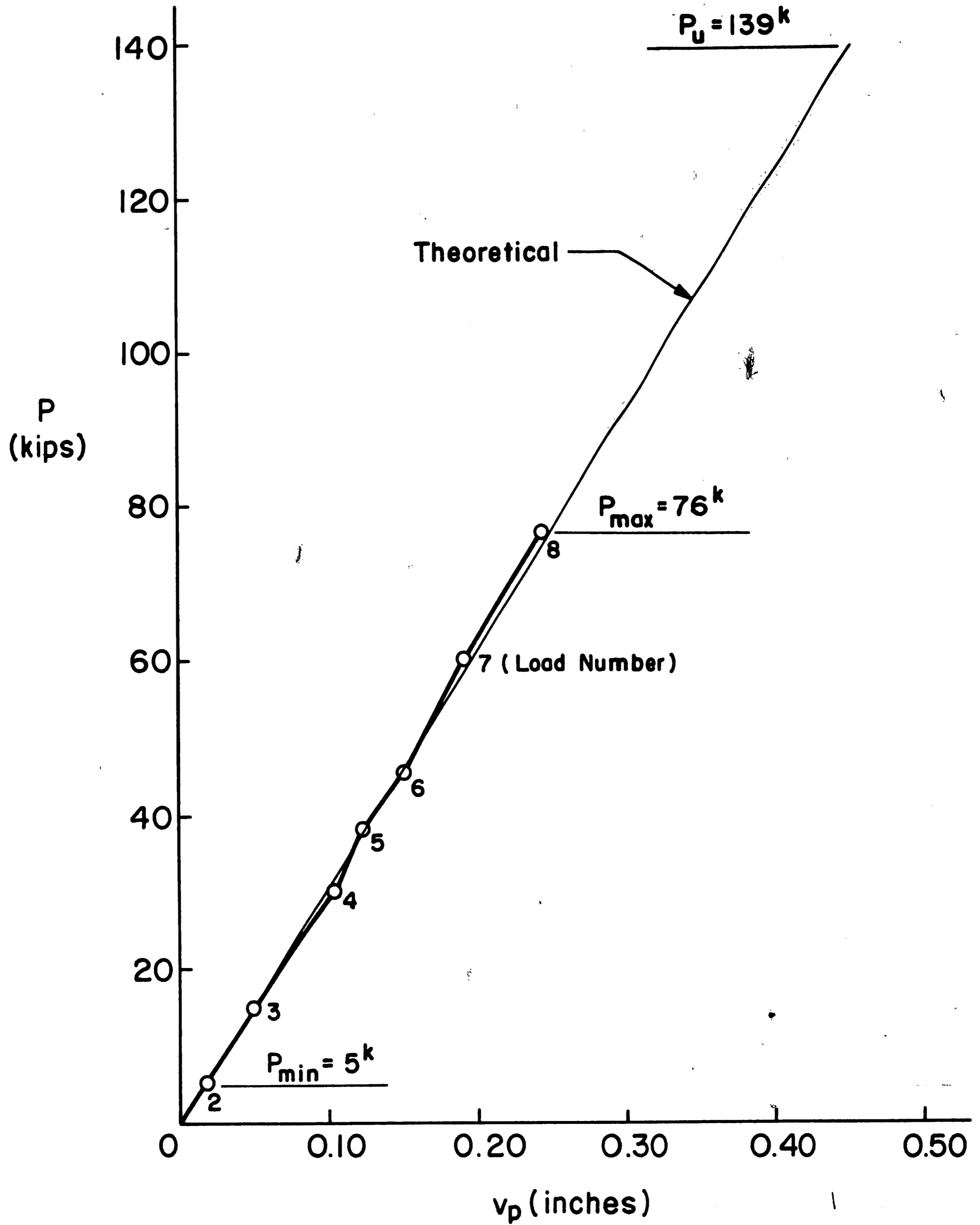
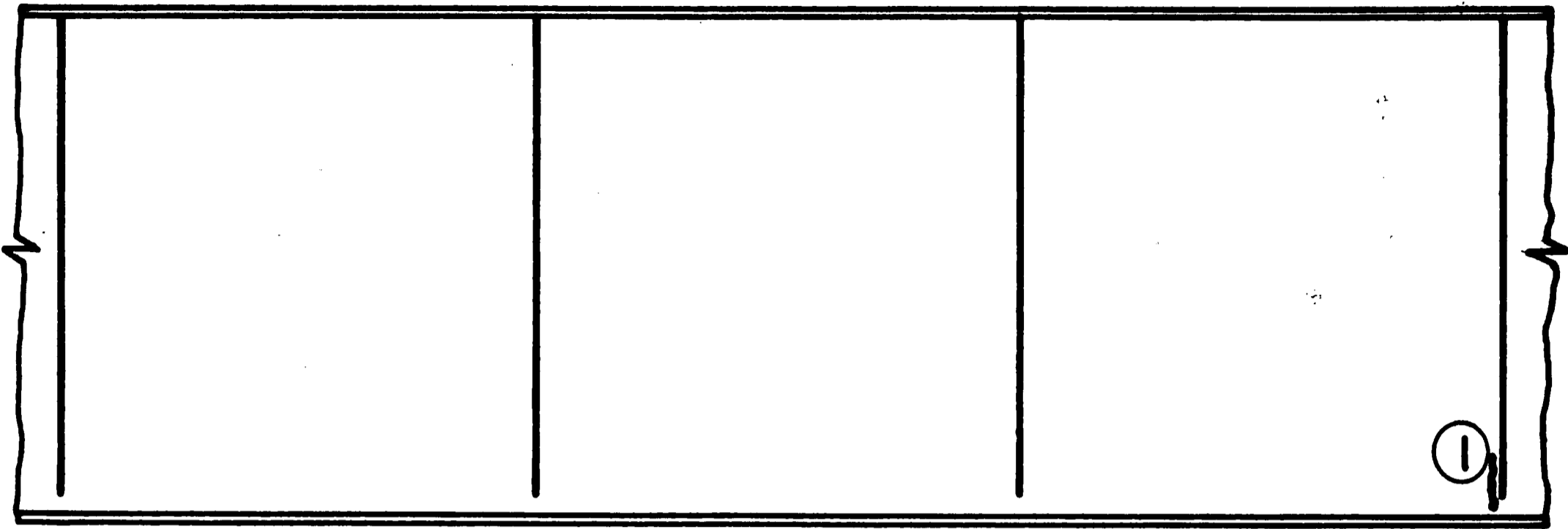
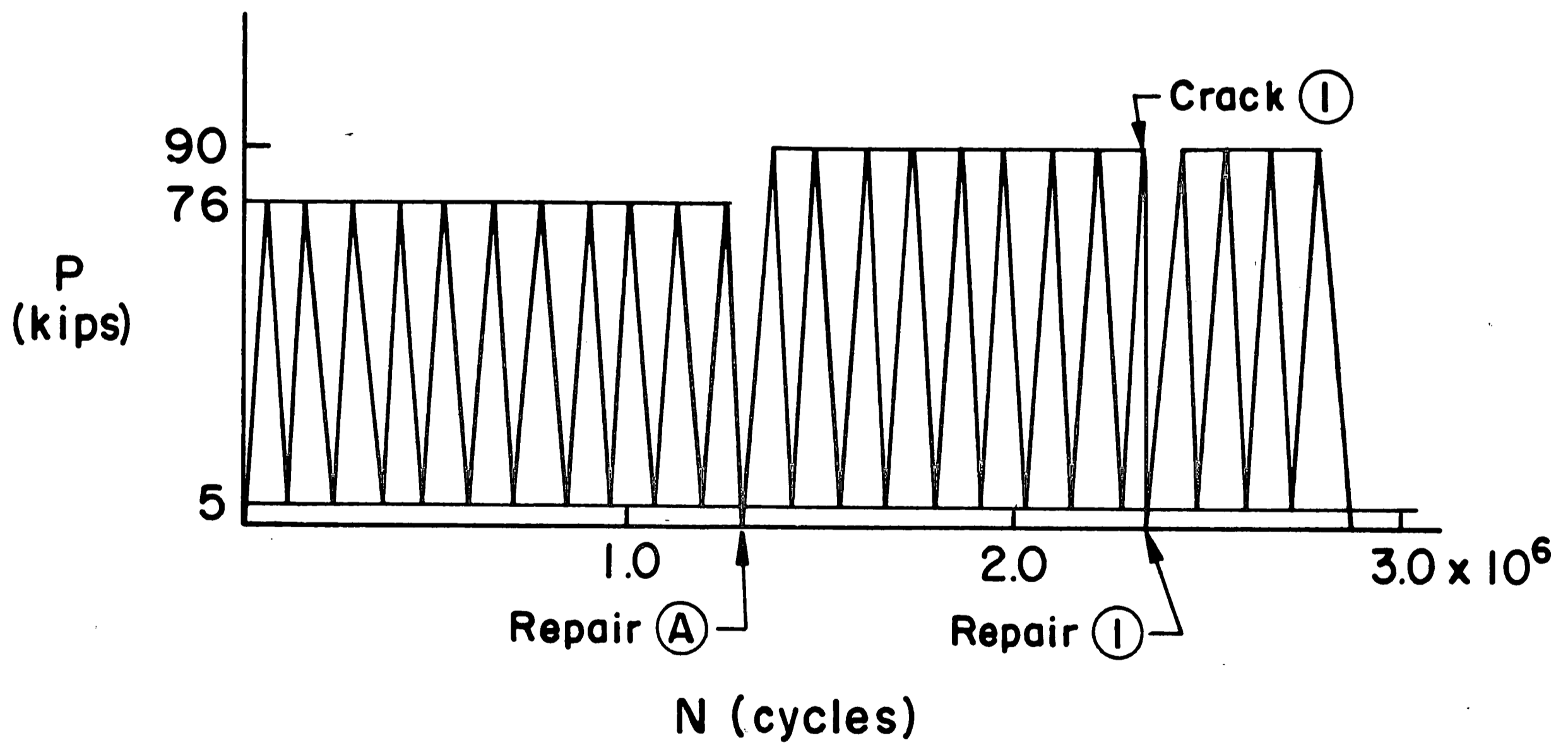


Fig. 7 Static Load Versus Deflection, Girder F7



(a) Crack Location



(b) Fatigue Test Sequence

Fig. 8 Fatigue Testing of Girder F7

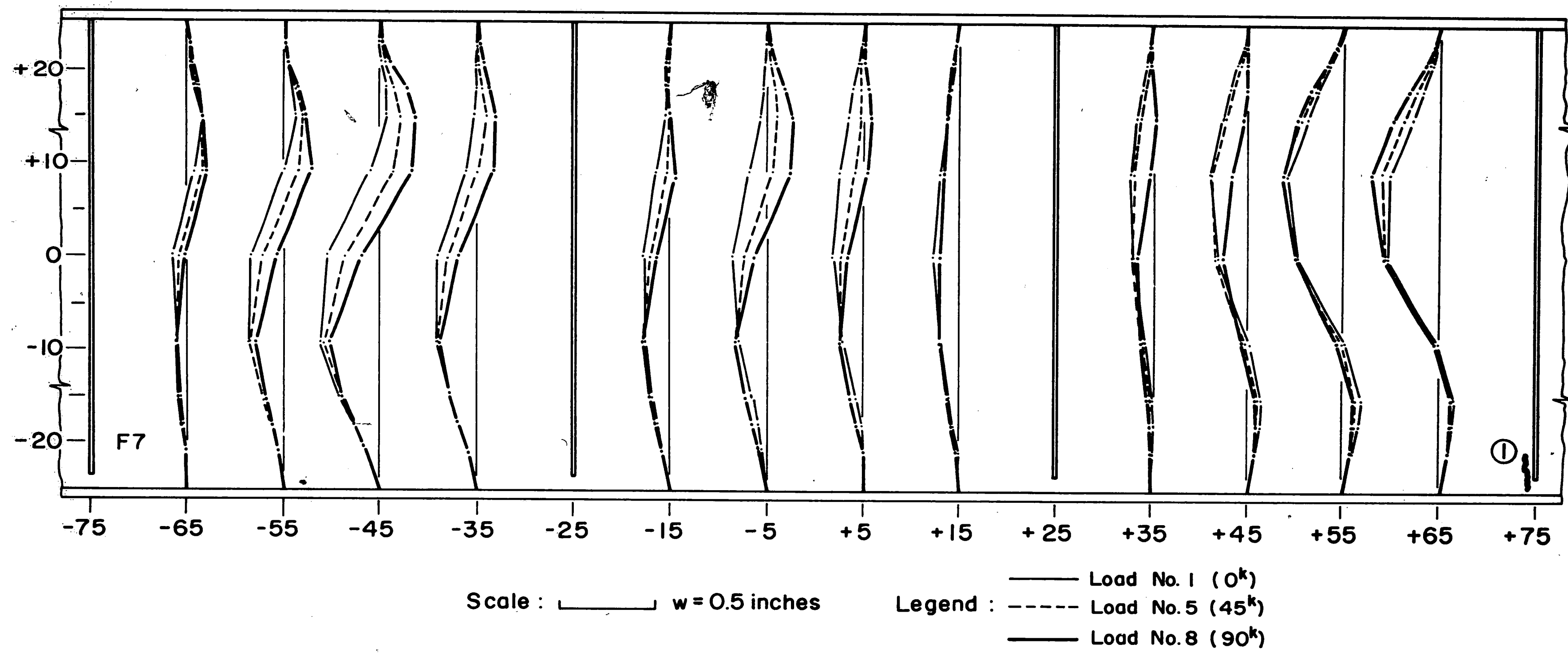


Fig. 9 Web Cross-Sectional Shapes, Girder F7

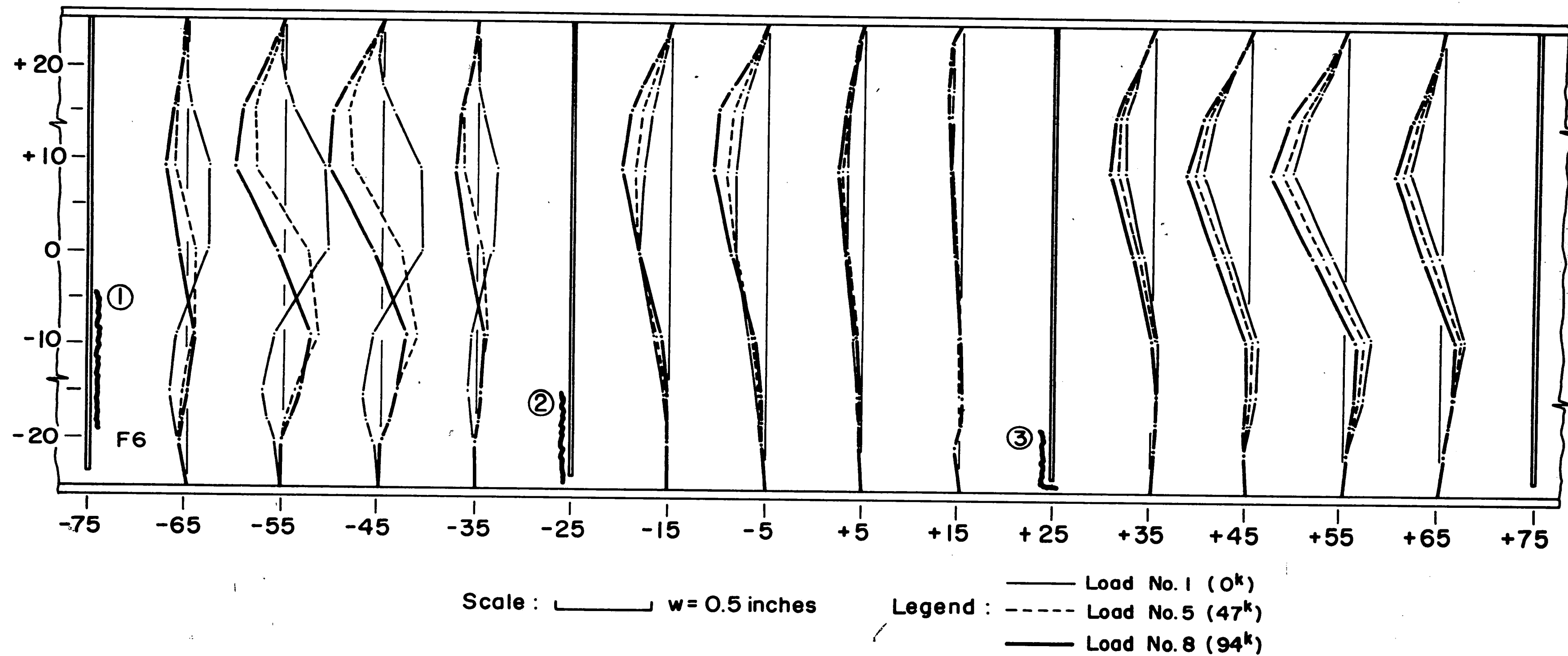
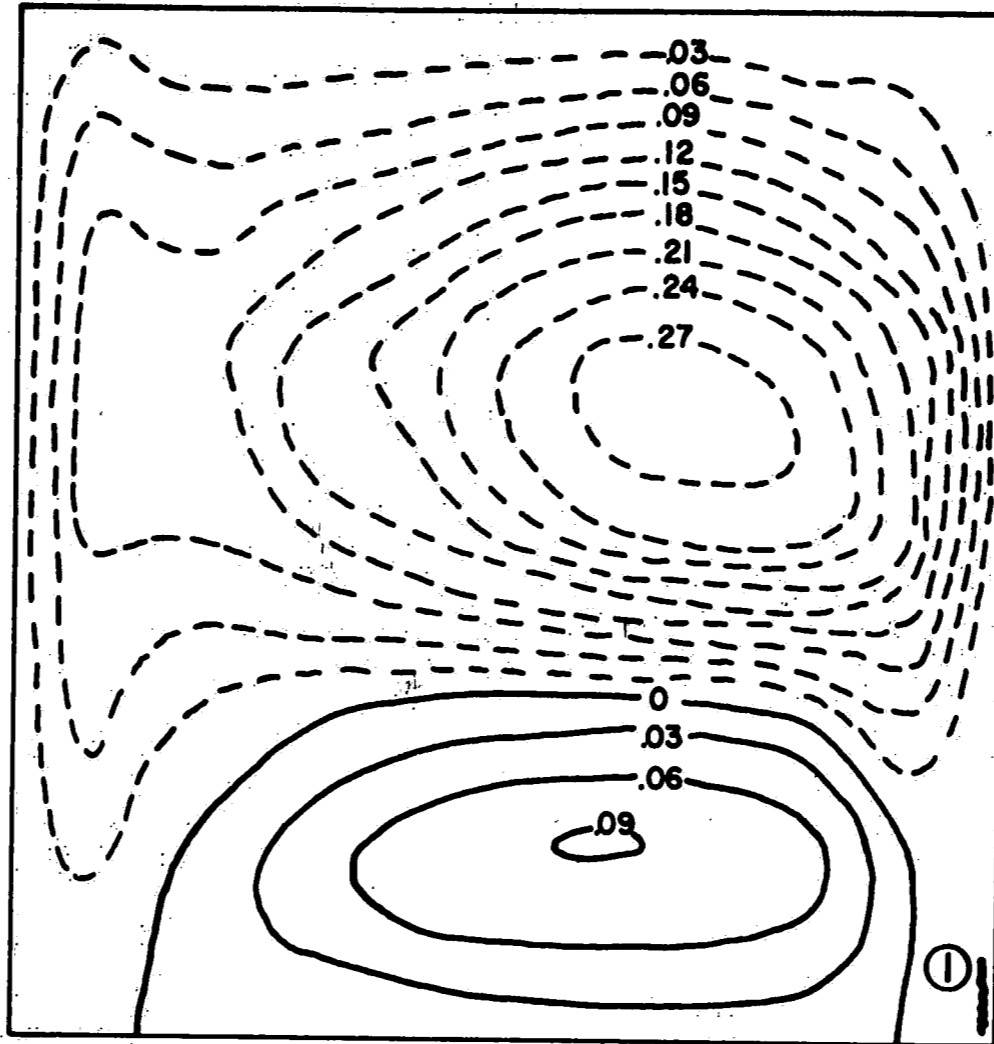
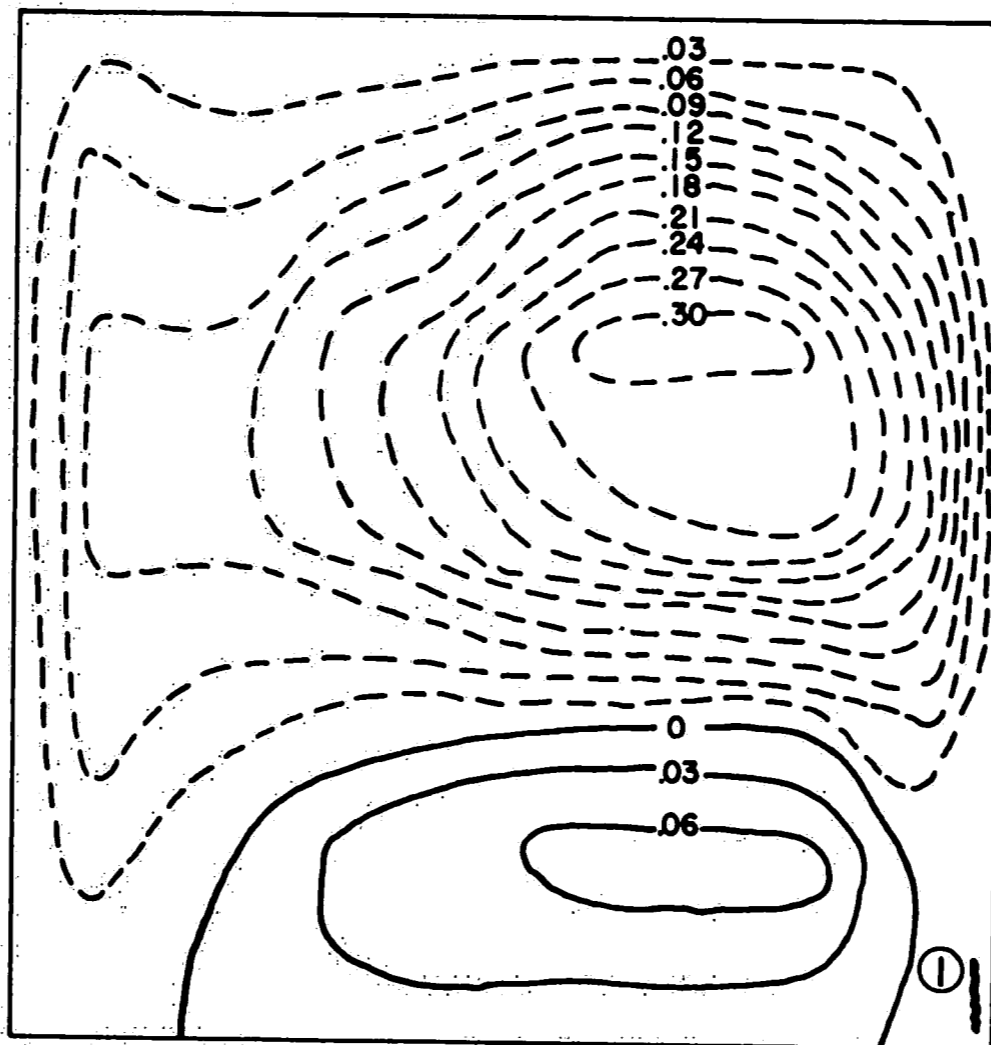


Fig. 10 Web Cross-Sectional Shapes, Girder F6

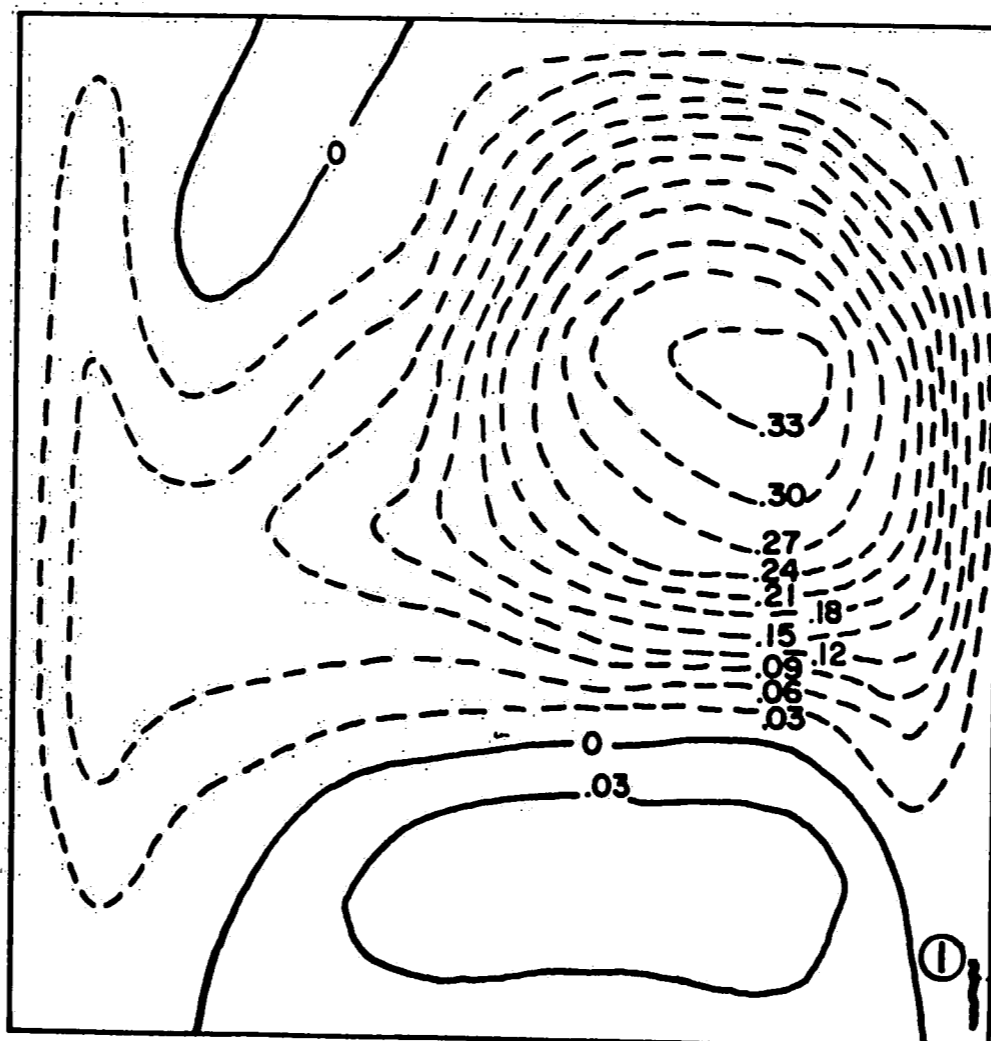


P = 0 kips  
LOAD No. 1

PANEL 3



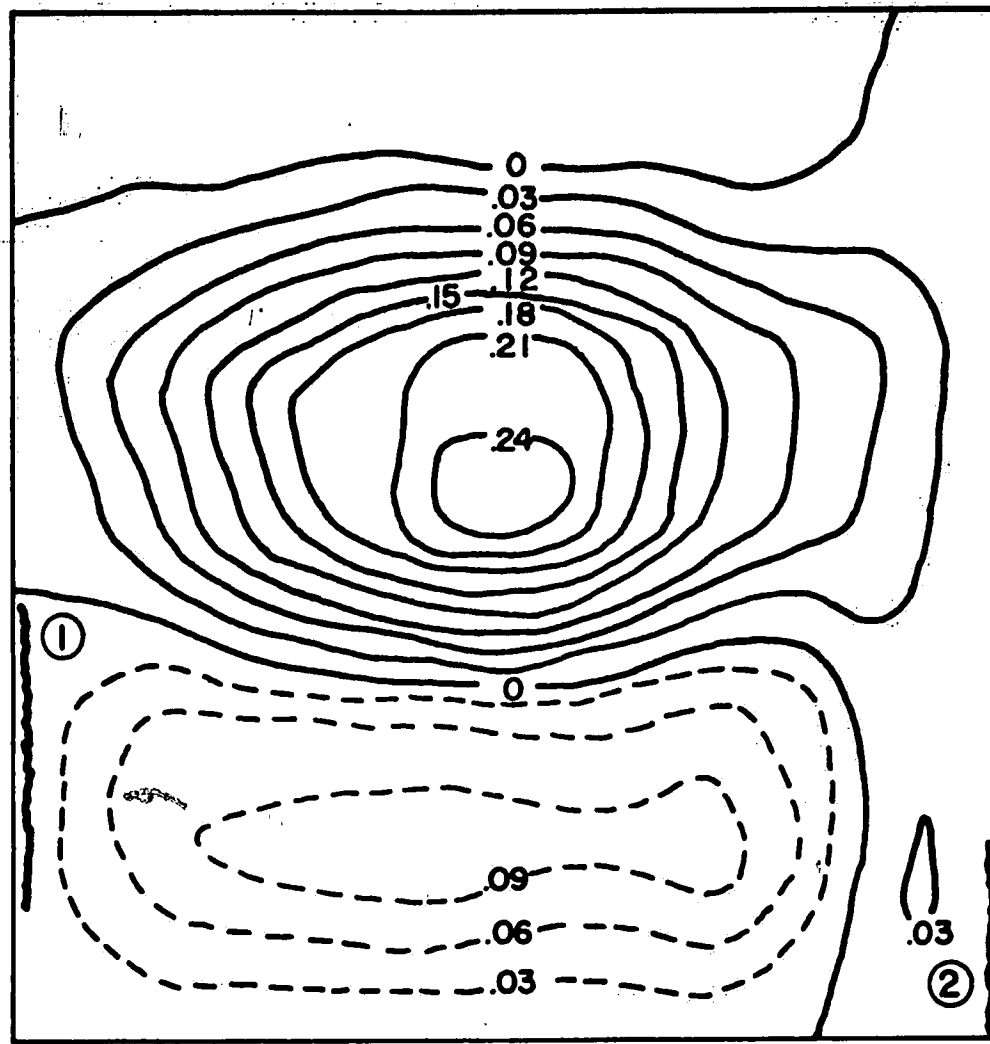
P = 45 kips  
LOAD No. 5



P = 90 kips  
LOAD No. 8

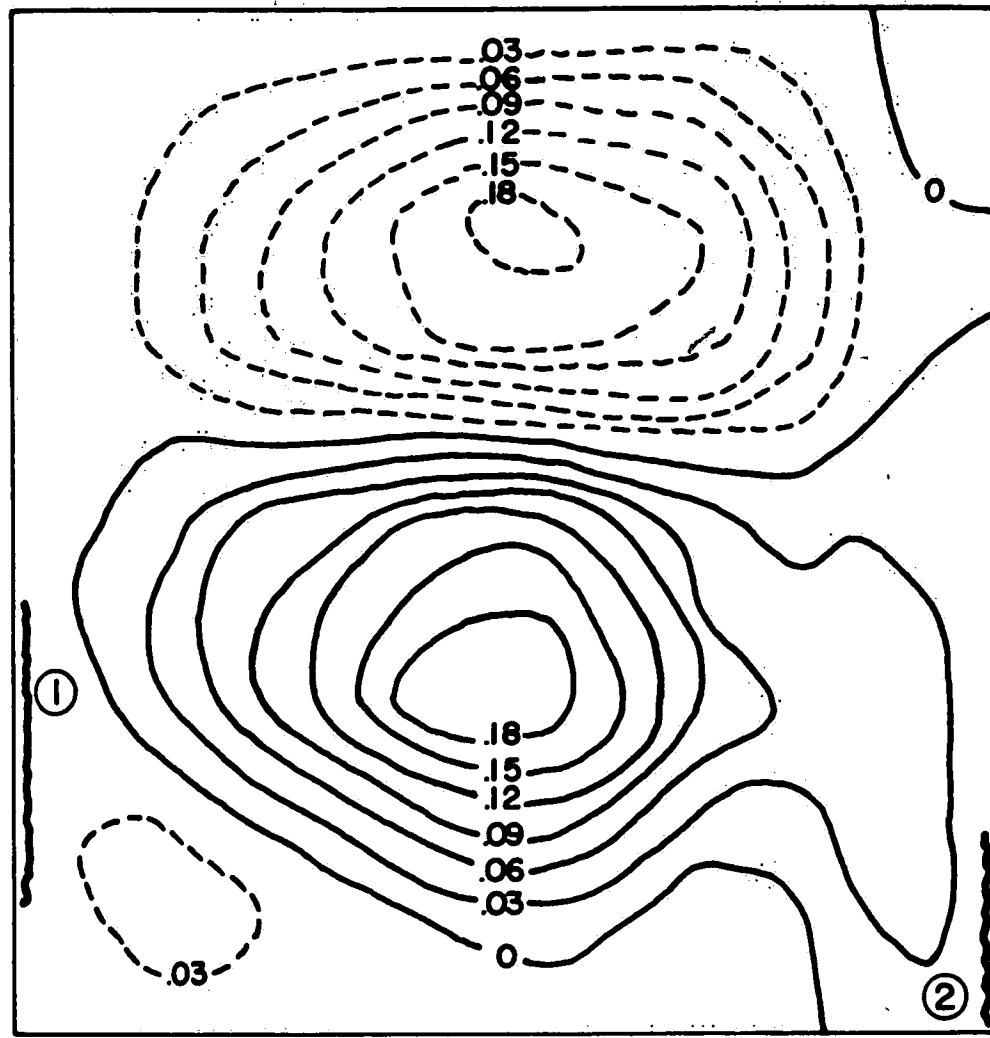
Fig. 11 Web Deflection Contours, Girder F7



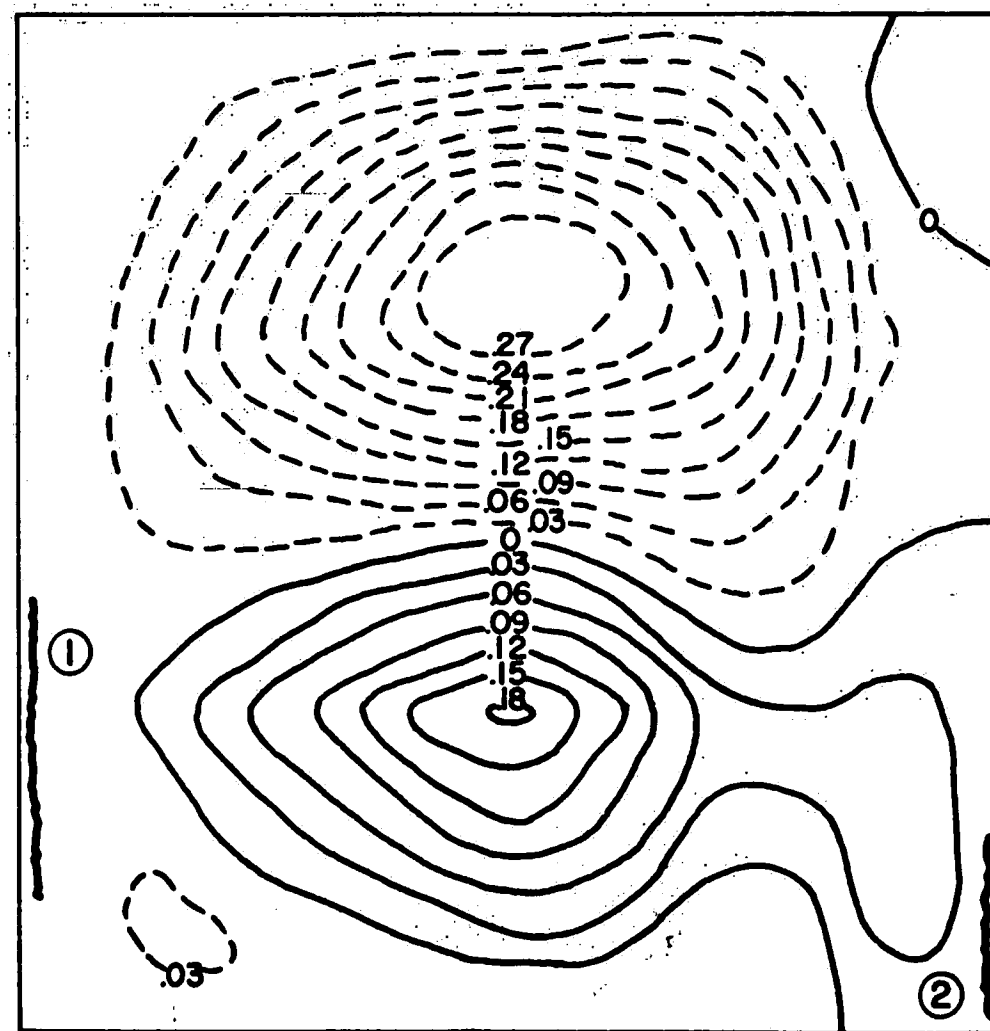


P = 0 kips  
LOAD No. 1

PANEL I



P = 47 kips  
LOAD No. 5



P = 94 kips  
LOAD No. 8

Fig. 12 Web Deflection Contours, Girder F6

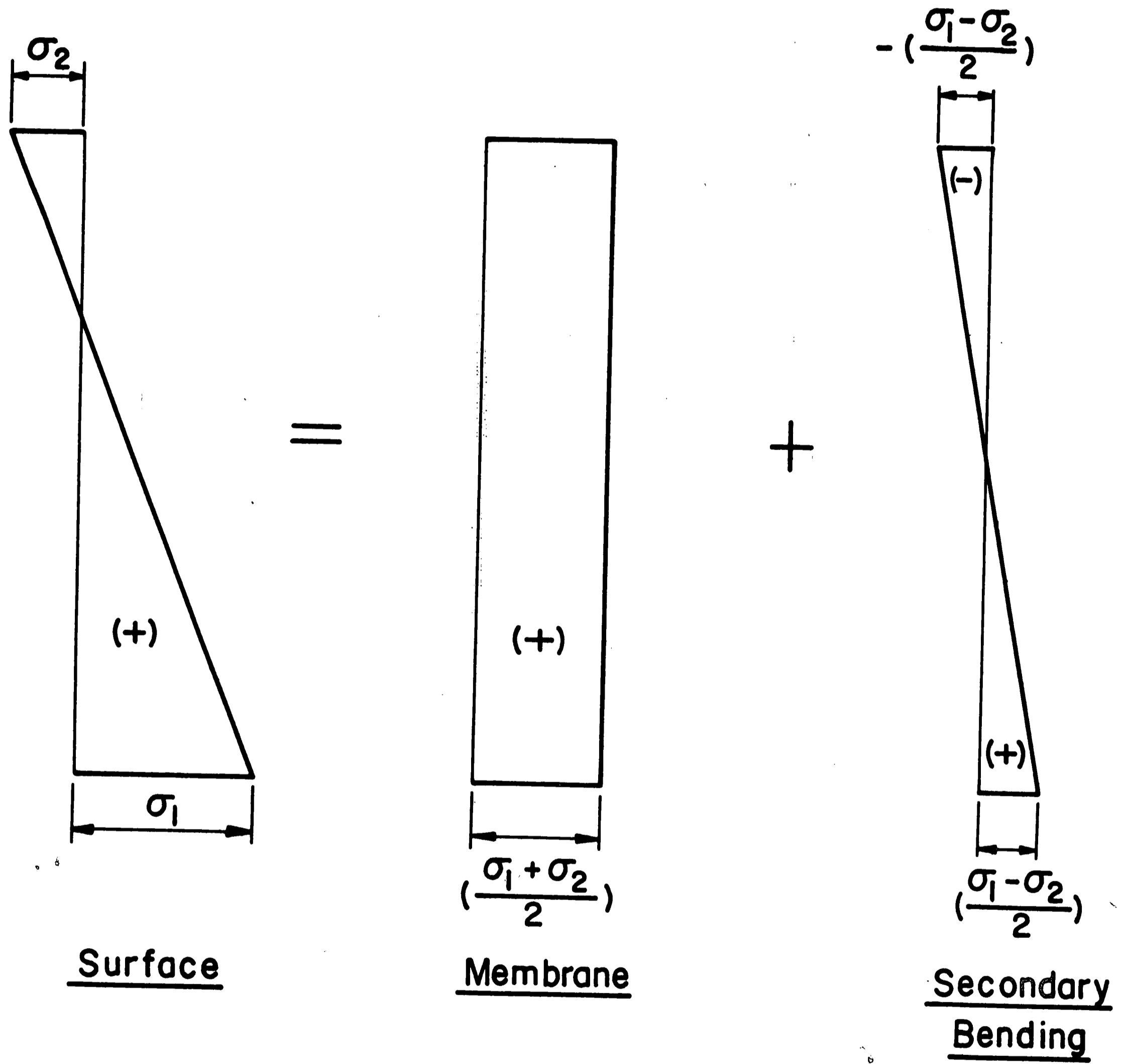
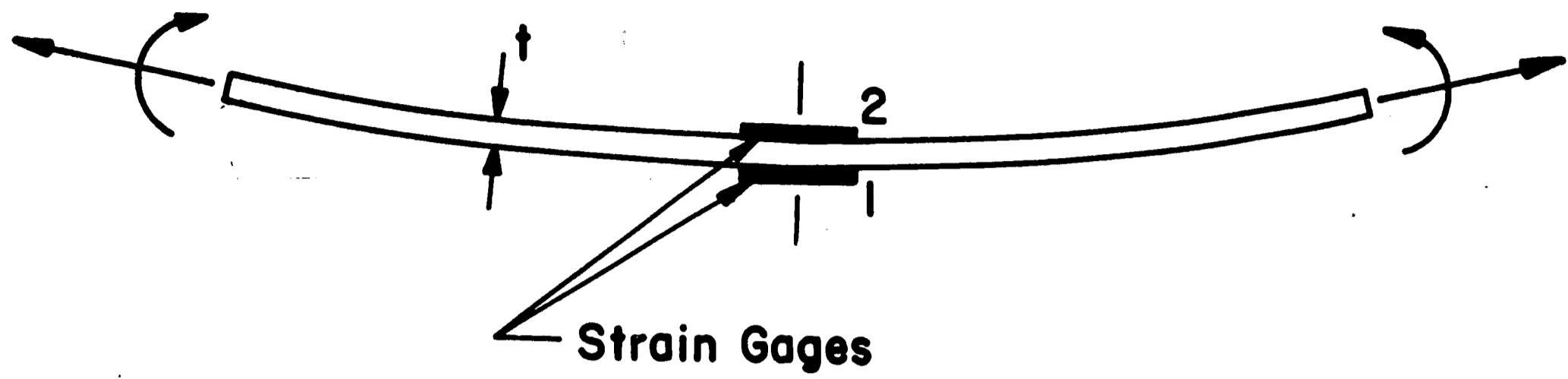
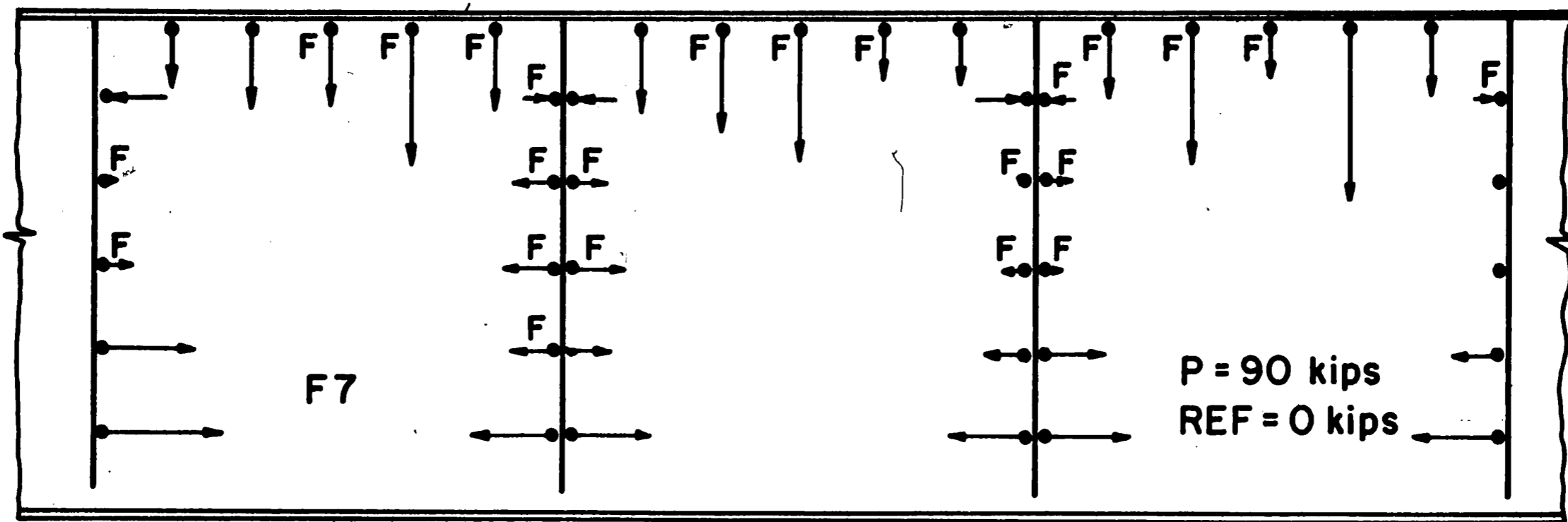
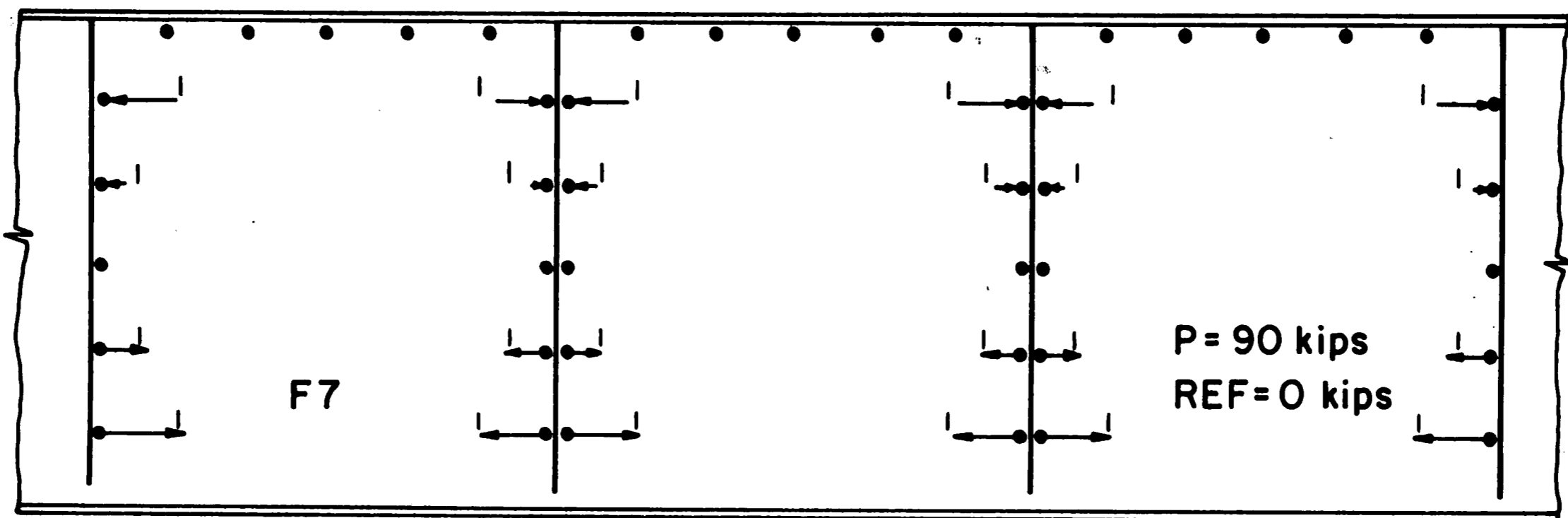


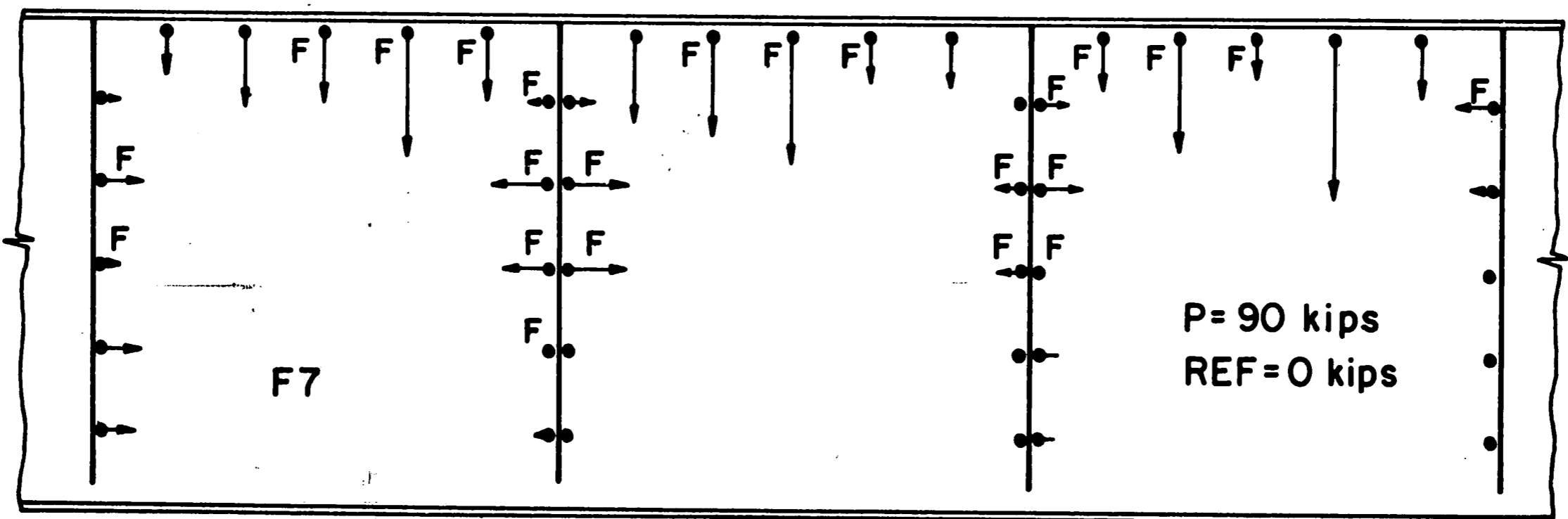
Fig. 13 Components of Surface Stress



(a) Surface Stress



(b) Membrane Stress

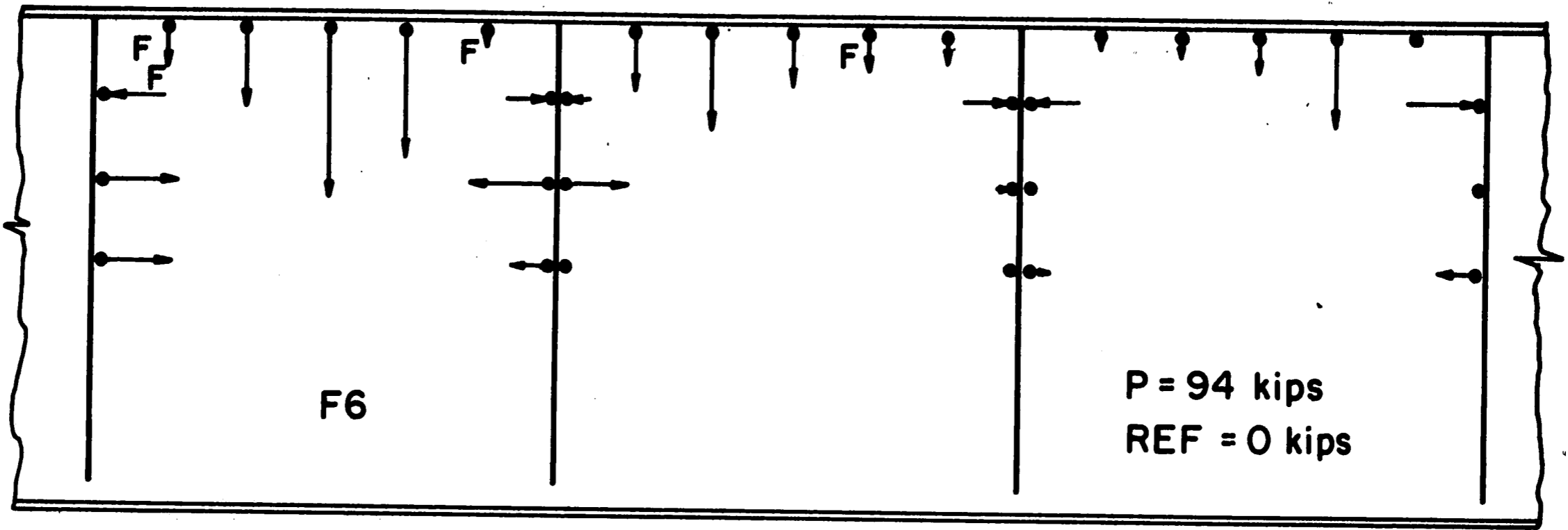


(c) Secondary Bending Stress

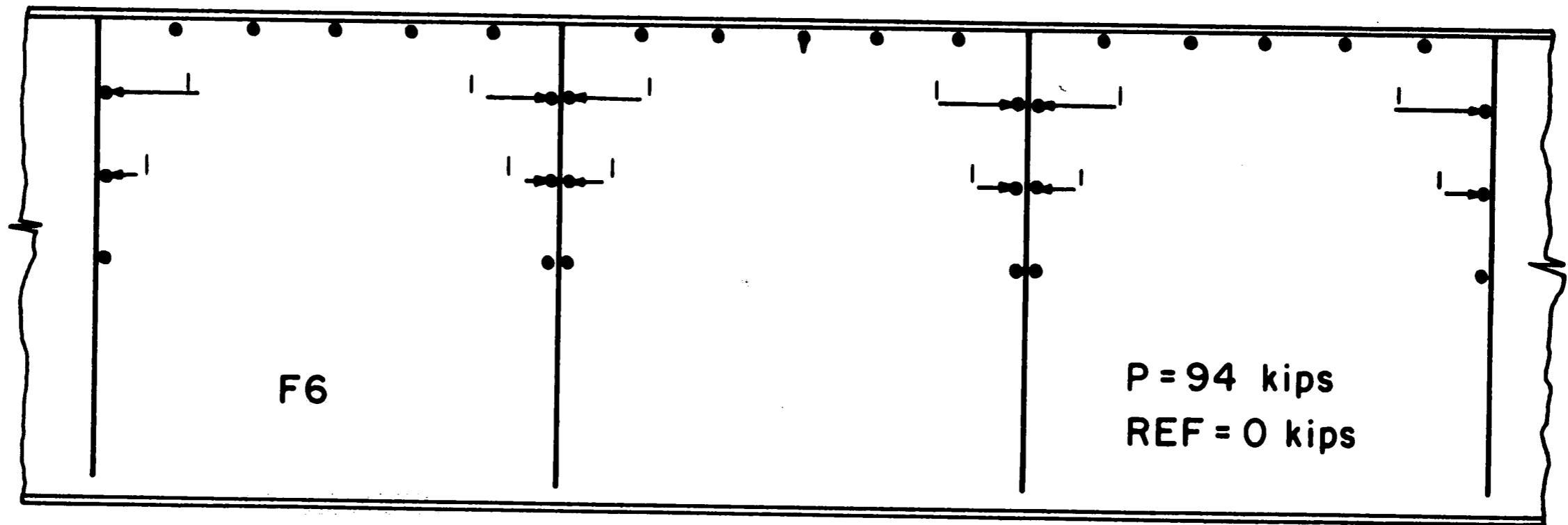
Scale : 0 20 (ksi)

Legend : Tension   
 Compression

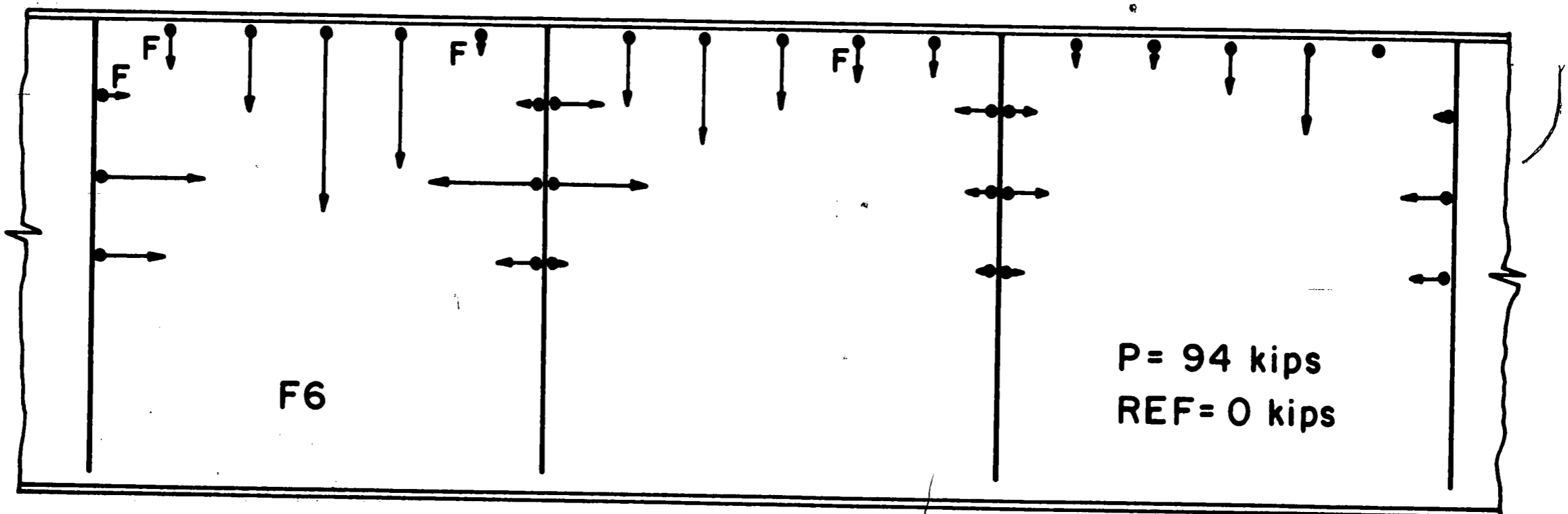
Fig. 14 Web Stresses Normal to the Boundary, Girder F7



(a) Surface Stress



(b) Membrane Stress

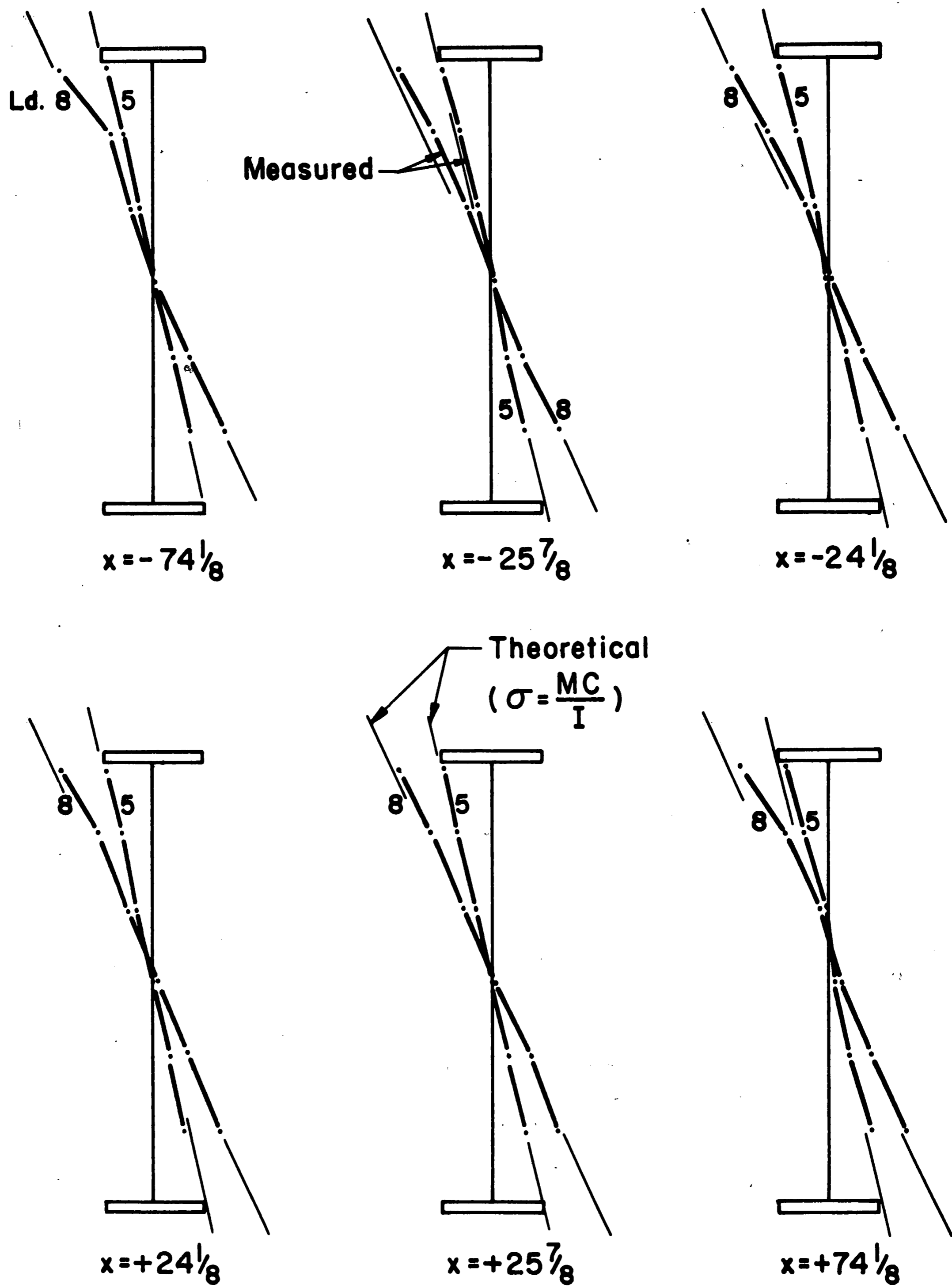


(c) Secondary Bending Stress

Scale : 0 20 (ksi)

Legend : Tension  
Compression

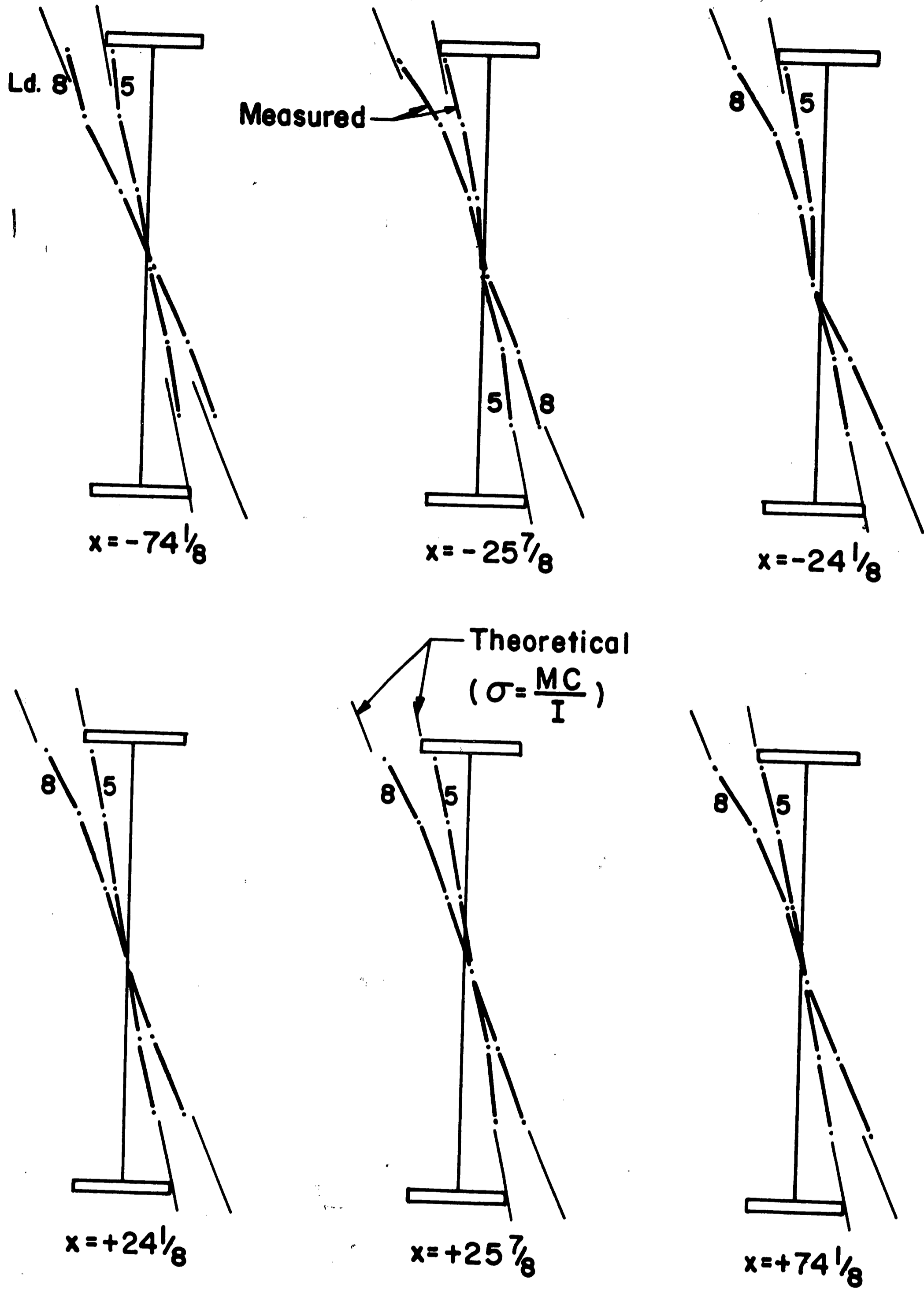
Fig. 15 Web Stresses Normal to the Boundary, Girder F6



Vertical Scale : 1" = 20"  
 Horizontal Scale : 1" = 30 ksi

Load 8 = 94 kips  
 Load 5 = 47 kips

Fig. 16 Cross-Sectional Distribution  
 of Web Membrane Stresses, Girder F6



Vertical Scale : 1" = 20"  
 Horizontal Scale : 1" = 30 ksi

Load 8 = 90 kips  
 Load 5 = 45 kips

Fig. 17 Cross-Sectional Distribution of Web Membrane Stresses, Girder F7

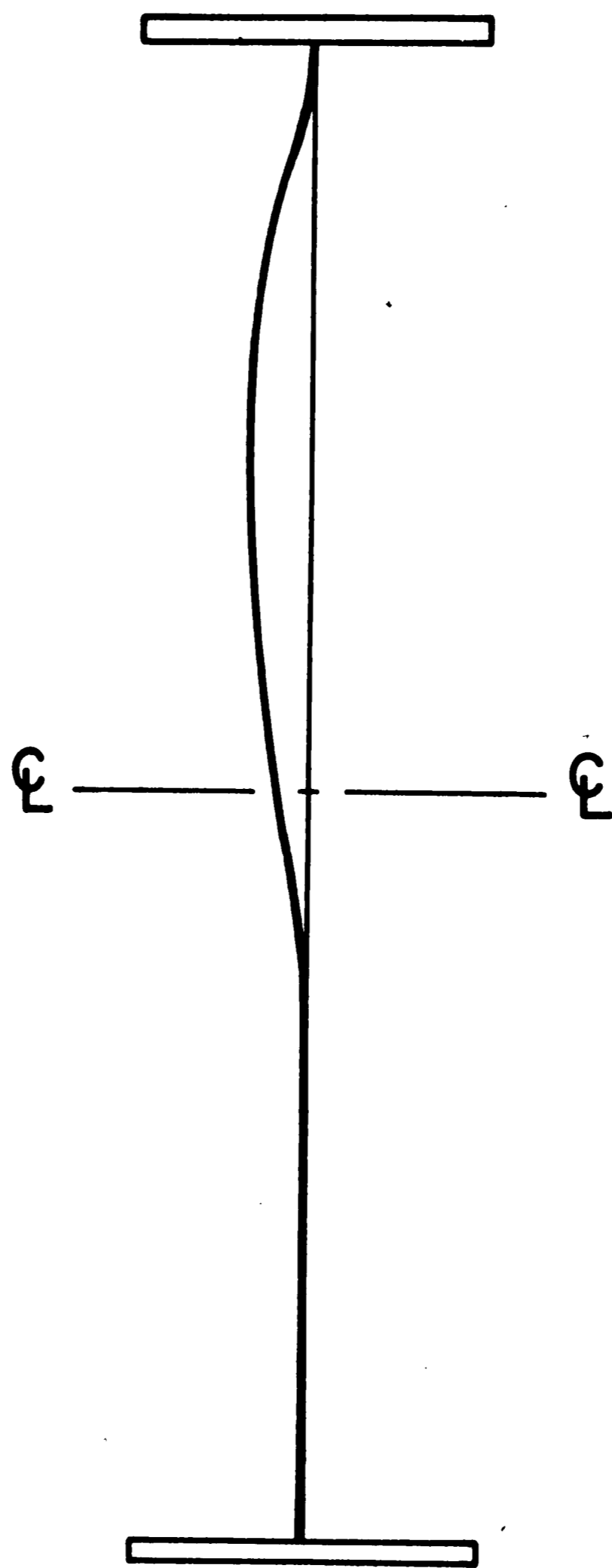


Fig. 18 Typical Web Deflection

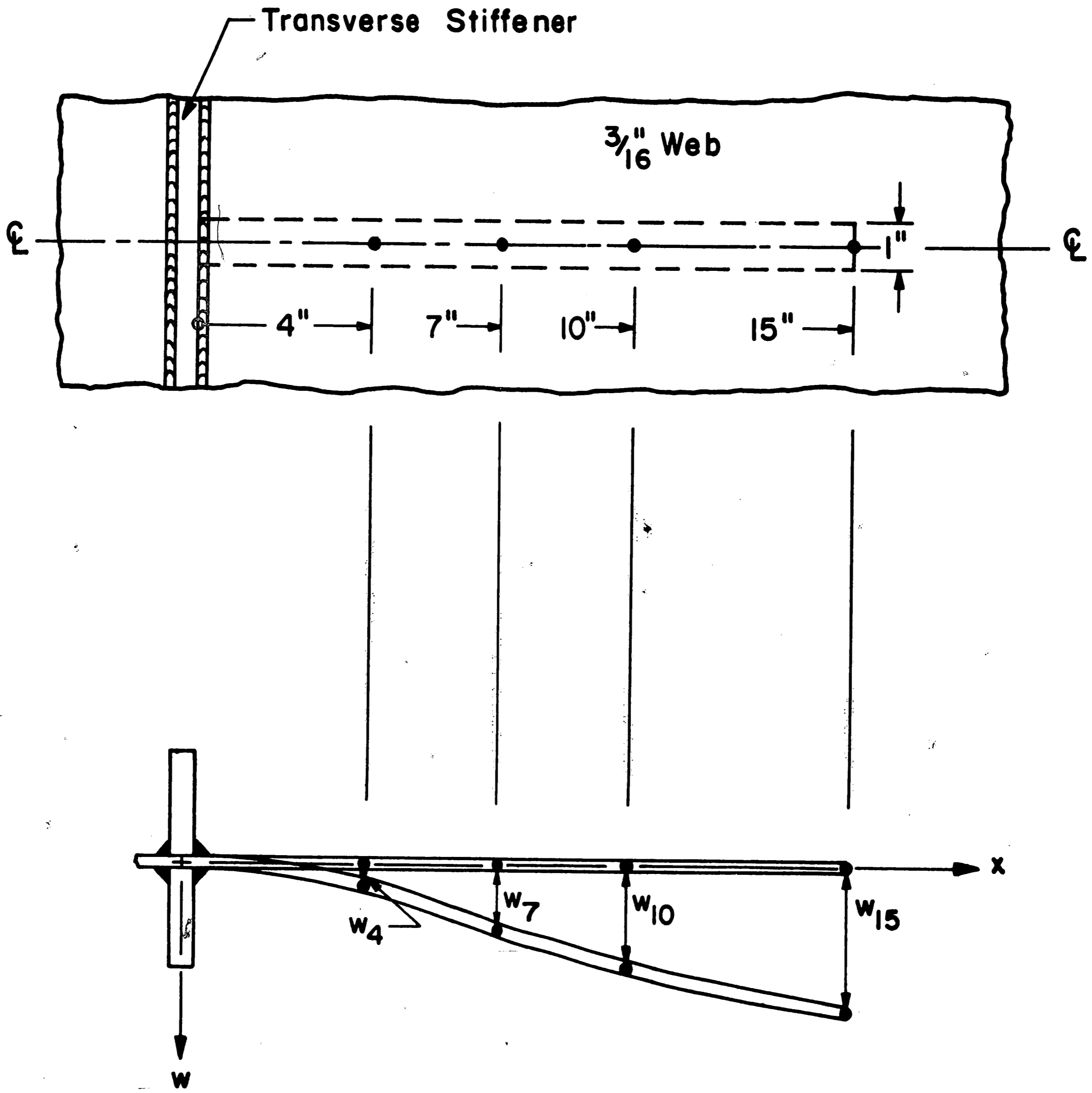
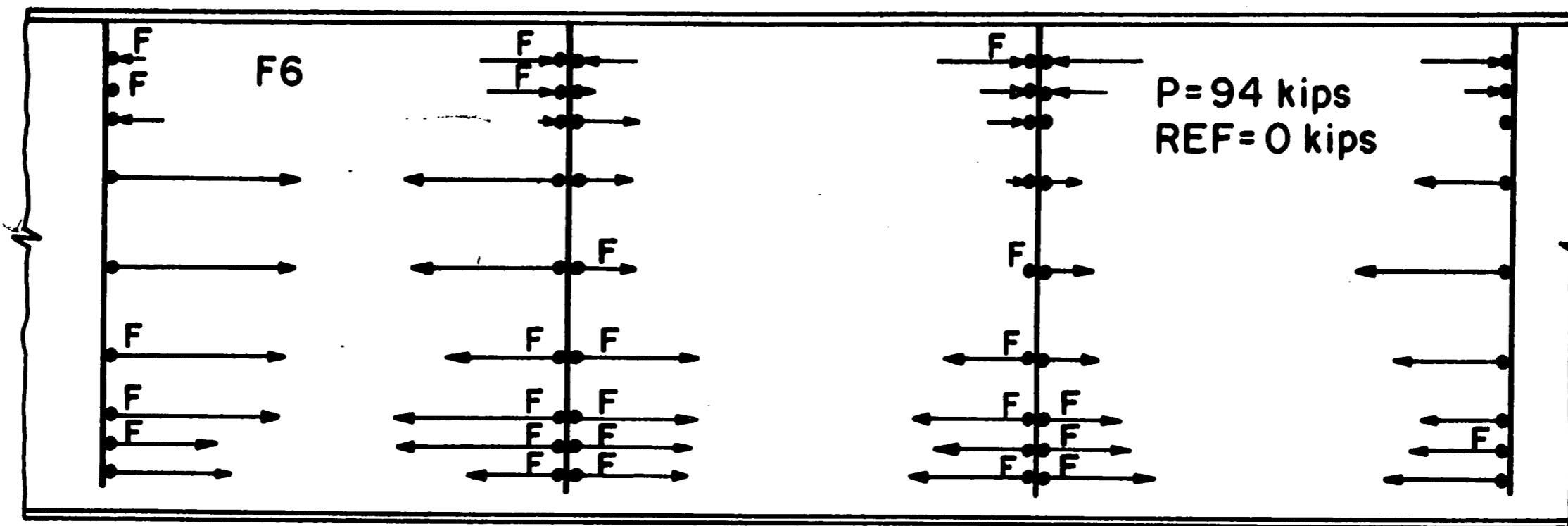
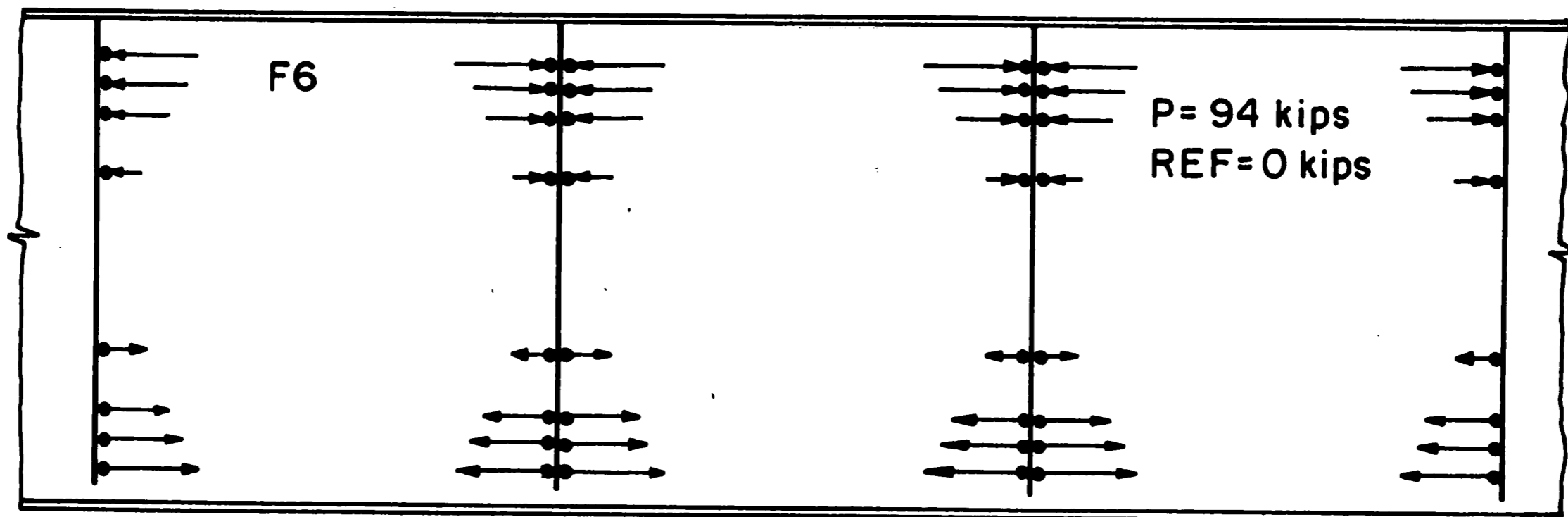


Fig. 19 Approximate Cantilever Strip

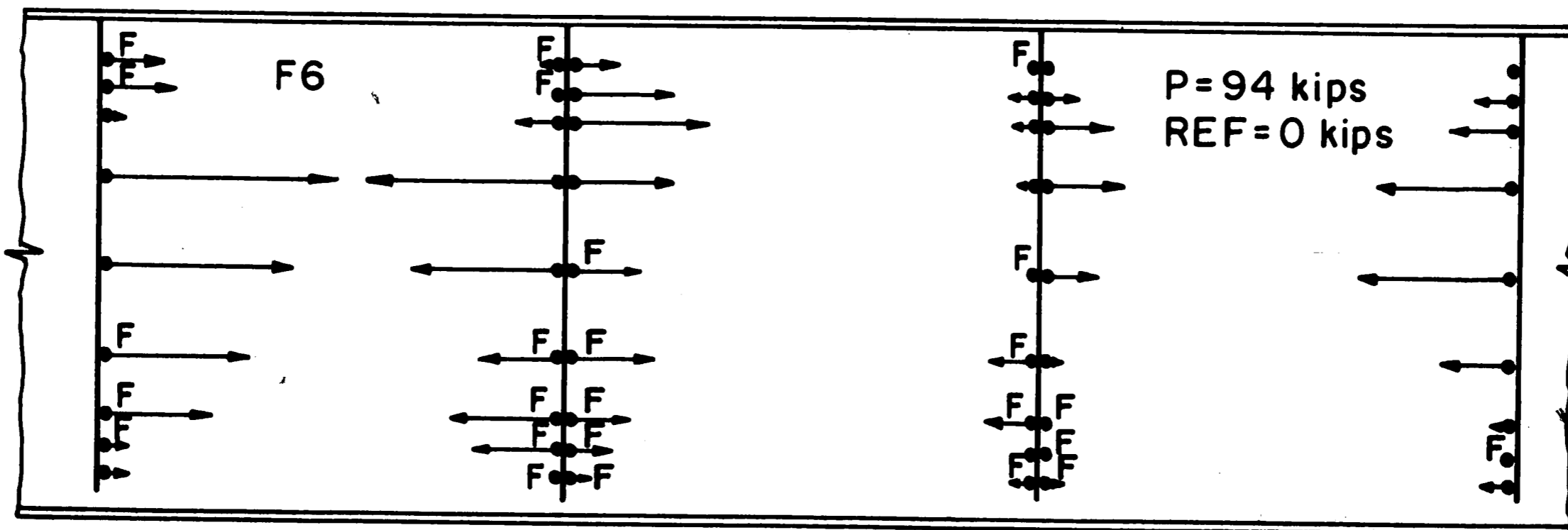




(a) Surface Stress



(b) Membrane Stress ( $\frac{MC}{I}$ )



(c) Secondary Bending Stress

Fig. 20 Approximate Web Stresses Normal to the Boundary, Girder F6

REFERENCES

1. K. Basler and B. Thurlimann  
STRENGTH OF PLATE GIRDERS IN BENDING,  
Proceedings, ASCE, Vol. 87, No. ST6, August 1961
2. K. Basler  
STRENGTH OF PLATE GIRDERS IN SHEAR,  
Proceedings, ASCE, Vol. 87, No. ST7, October 1961
3. K. Basler  
STRENGTH OF PLATE GIRDERS UNDER COMBINED BENDING AND SHEAR,  
Proceedings, ASCE, Vol. 87, No. ST7, October 1961
4. K. Basler, B. T. Yen, J. A. Mueller, and B. Thurlimann  
WEB BUCKLING TESTS ON WELDED PLATE GIRDERS,  
Bulletin No. 64, Welding Research Council, New York,  
September 1960
5. B. T. Yen and J. A. Mueller  
FATIGUE TESTS OF WELDED PLATE GIRDERS IN SHEAR,  
Lehigh University, Fritz Engineering Laboratory Report No.  
303.6, November 1964
6. W. E. Fisher and J. E. Stallmeyer  
BEHAVIOR OF WELDED BUILT-UP BEAMS UNDER REPEATED LOADS,  
University of Illinois, Structural Research Series No. 147,  
March 1958
7. W. H. Munse and L. Grover  
FATIGUE OF WELDED STEEL STRUCTURES,  
Welding Research Council, New York, 1964
8. N. G. Kouba and J. E. Stallmeyer  
THE BEHAVIOR OF STIFFENED BEAMS UNDER REPEATED LOADS,  
University of Illinois, Structural Research Series No. 173,  
April 1959
9. Welded Research Council  
FATIGUE TESTS OF BEAMS IN FLEXURE,  
March 1951

VITA

The author was born in Hoboken, New Jersey, December 9, 1940, the fourth child of Josephine (Castagnetti) and Alphonse Corrado.

He was graduated from Demarest High School in Hoboken, New Jersey, in January 1958. He then attended St. Bonaventure University in Olean, New York from September 1958 to June 1960. In September 1960 he enrolled at the University of Detroit, Detroit, Michigan and in June 1963 received the degree of Bachelor of Civil Engineering from the same university.

The author married the former Arlene Margaret Collins on December 2, 1961. They have since been blessed with a son, Joseph James.

He was awarded a Research Assistantship in Civil Engineering at Fritz Engineering Laboratory, Lehigh University, Bethlehem, Pennsylvania and began studies for a Master's Degree in September 1963. The author has been associated with the research concerning the fatigue strength of welded plate girders.